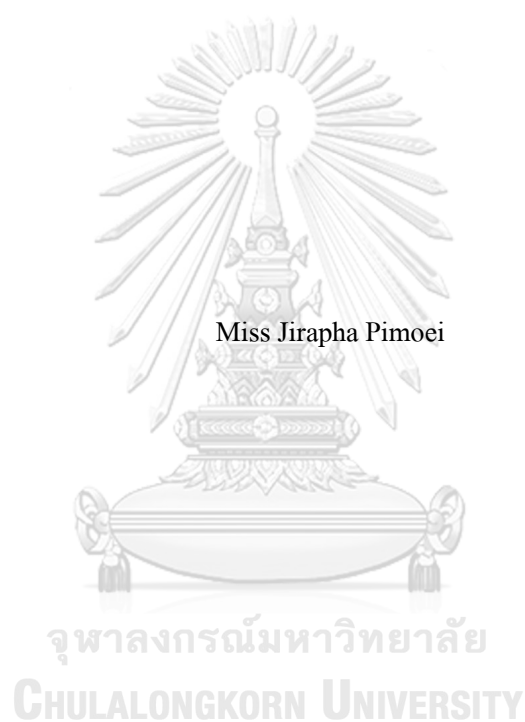


IODINE ENCAPSULATION USING ANIONIC POLYELECTROLYTES FOR
RECHARGEABLE ZINC-IODINE BATTERIES



Miss Jirapha Pimoei

A Thesis Submitted in Partial Fulfillment of the Requirements
for the Degree of Master of Engineering in Chemical Engineering

Department of Chemical Engineering

FACULTY OF ENGINEERING

Chulalongkorn University

Academic Year 2019

Copyright of Chulalongkorn University

การพ่นกั๊มไอโอดีนโดยใช้พอลิอิเล็กโทรไลต์ที่มีประจุลบ สำหรับแบตเตอรี่สังกะสี-ไอโอดีนแบบ
ชาร์จซ้ำได้



วิทยานิพนธ์นี้เป็นส่วนหนึ่งของการศึกษาตามหลักสูตรปริญญาวิศวกรรมศาสตรมหาบัณฑิต
สาขาวิชาวิศวกรรมเคมี ภาควิชาวิศวกรรมเคมี
คณะวิศวกรรมศาสตร์ จุฬาลงกรณ์มหาวิทยาลัย
ปีการศึกษา 2562
ลิขสิทธิ์ของจุฬาลงกรณ์มหาวิทยาลัย

Thesis Title IODINE ENCAPSULATION USING ANIONIC
POLYELECTROLYTES FOR RECHARGEABLE ZINC-
IODINE BATTERIES

By Miss Jirapha Pimoei

Field of Study Chemical Engineering

Thesis Advisor Associate Professor ANONGNAT SOMWANGTHANAROJ,
Ph.D.

Thesis Co Advisor JITTI KASEMCHAINAN, Ph.D.

Accepted by the FACULTY OF ENGINEERING, Chulalongkorn University in Partial
Fulfillment of the Requirement for the Master of Engineering

..... Dean of the FACULTY OF
ENGINEERING
(Professor SUPOT TEACHAVORASINSKUN, D.Eng.)

THESIS COMMITTEE

..... Chairman
(CHUTIMON SATIRAPIATHKUL, Ph.D.)

..... Thesis Advisor
(Associate Professor ANONGNAT SOMWANGTHANAROJ,
Ph.D.)

..... Thesis Co-Advisor
(JITTI KASEMCHAINAN, Ph.D.)

..... Examiner
(Associate Professor SOORATHEP KHEAWHOM, Ph.D.)

..... External Examiner
(Assistant Professor Pornchai Bumroongsri, D.Eng.)

จิราภา พิเมย : การผนึกหุ้มไอโอดีนโดยใช้พอลิอิเล็กโทรไลต์ที่มีประจุลบ สำหรับ
 แบตเตอรี่สังกะสี-ไอโอดีนแบบชาร์จซ้ำได้. (IODINE ENCAPSULATION USING
 ANIONIC POLYELECTROLYTES FOR RECHARGEABLE ZINC-IODINE
 BATTERIES) อ.ที่ปรึกษาหลัก : รศ. ดร.อนงค์นาฏ สมหวังชนโรจน์, อ.ที่ปรึกษาร่วม :
 ดร.จิตติ เกษมชัยนันท์

แบตเตอรี่สังกะสี - ไอโอดีนแบบชาร์จซ้ำได้นั้นเป็นที่น่าสนใจสำหรับการนำมาทำ
 อุปกรณ์จัดเก็บพลังงานไฟฟ้าเนื่องจากองค์ประกอบของแบตเตอรี่ชนิดนี้เป็นทรัพยากรที่มี
 มากมาย, ต้นทุนต่ำ, และมีความปลอดภัยสูง อย่างไรก็ตามแบตเตอรี่เหล่านี้ยังคงมีปัญหาบาง
 ประการ เช่น ความเสถียรในการไซเคิลที่ยังไม่ดีและการคายประจุด้วยตัวเองสูง เนื่องมาจากการ
 รั่วไหลของอนุพันธ์ไอโอดีนจากขั้วบวก ซึ่งการใช้พอลิอิเล็กโทรไลต์ประจุลบเป็นสารยึดเกาะ
 ช่วยเพื่อบรรเทาปัญหานี้เพราะพอลิอิเล็กโทรไลต์ประจุลบเหล่านี้สามารถที่จะผนึกหุ้มไอโอดีน
 และช่วยให้การถ่ายโอนไอออนที่สำคัญต่อการเกิดปฏิกิริยาผ่านได้สะดวก ในงานวิจัยนี้ได้
 ทำการศึกษาพอลิอิเล็กโทรไลต์ประจุลบชนิดต่างๆ ได้แก่ โซเดียมคาร์บอกซิเมทิลเซลลูโลส (Na-
 CMC) โซเดียมอัลจินต (Na-Alg) และ โซเดียมพอลิสไตรีนซัลโฟเนต (Na-PSS) แบตเตอรี่ถูก
 ประดิษฐ์ขึ้นเป็นแบบเซลล์ CR2025 เพื่อตรวจสอบประสิทธิภาพทางเคมีไฟฟ้า ผลการวิจัยแสดง
 ให้เห็นว่าอิเล็กโทรดบวกที่เตรียมจากการใช้พอลิอิเล็กโทรไลต์ประจุลบเหล่านี้เป็นสารยึดเกาะ
 ช่วย สามารถทำให้ความสามารถในการใช้กระแสที่อัตราสูงมีค่าที่ดีมากและสามารถปรับปรุง
 ความจุจำเพาะได้มากถึง $127.37 \text{ mAh g}^{-1}$ ถ้าใช้สารยึดเกาะเป็น PVA-NaCMC ในขณะที่ใช้สาร
 ยึดเกาะเป็น PVA จะให้ค่าเพียง $104.06 \text{ mAh g}^{-1}$ นอกจากนี้พอลิอิเล็กโทรไลต์ประจุลบเหล่านี้
 สามารถผนึกหุ้มอนุพันธ์ไอโอดีนในขั้วไฟฟ้าบวกได้มากกว่าการใช้สารยึดเกาะ PVA ส่งผลให้มี
 อัตราการคายประจุด้วยตัวเองมีค่าต่ำ ดังนั้นขั้วไฟฟ้าบวกที่มีพอลิอิเล็กโทรไลต์ประจุลบเหล่านี้
 เป็นสารยึดเกาะช่วยนั้น จึงมีแนวโน้มที่น่าสนใจสำหรับการทำขั้วบวกในแบตเตอรี่สังกะสี -
 ไอโอดีนแบบชาร์จซ้ำได้

สาขาวิชา วิศวกรรมเคมี
 ปีการศึกษา 2562

ลายมือชื่อนิสิต
 ลายมือชื่อ อ.ที่ปรึกษาหลัก
 ลายมือชื่อ อ.ที่ปรึกษาร่วม

6170127321 : MAJOR CHEMICAL ENGINEERING

KEYWORD: Zinc-iodine batteries, Anionic polyelectrolytes, Sodium carboxymethyl cellulose, Sodium alginate, Sodium polystyrene sulfonate, polyvinyl alcohol (PVA)

Jirapha Pimoei : IODINE ENCAPSULATION USING ANIONIC POLYELECTROLYTES FOR RECHARGEABLE ZINC-IODINE BATTERIES.

Advisor: Assoc. Prof. ANONGNAT SOMWANGTHANAROJ, Ph.D. Co-advisor: JITTI KASEMCHAINAN, Ph.D.

Rechargeable zinc-iodine batteries are attractive as promising candidates for electrical energy storage due to their abundant resources, low cost, and high safety. However, these batteries still have some problems, such as poor cycling stability and high self-discharge due to the leakage of iodine species from the positive electrode. Anionic polyelectrolytes can be applied as supportive binders to alleviate this issue because these polyelectrolytes can encapsulate iodine species and facilitate the transfer of other active species. In this study, different types of anionic polyelectrolytes, including sodium carboxymethyl cellulose (Na-CMC), sodium alginate (Na-Alg), and sodium polystyrene sulfonate (Na-PSS), were investigated. The batteries were fabricated in CR2025 cells to investigate the electrochemical performance. The results showed that the positive electrodes processed with these anionic polyelectrolytes as supportive binders could show remarkable high-rate capability and improve specific capacity reach to $127.37 \text{ mAh g}^{-1}$, which used PVA-NaCMC binder while it only $104.06 \text{ mAh g}^{-1}$ when using a PVA binder. Additionally, these anion polyelectrolytes can encapsulate iodine species in positive electrodes better than a PVA binder leading to a low self-discharge rate. Therefore, positive electrodes with these anionic polyelectrolytes as supportive binders are promising binders for the positive electrode in the rechargeable zinc-iodine batteries.

Field of Study: Chemical Engineering

Student's Signature

Academic Year: 2019

Advisor's Signature

Co-advisor's Signature

ACKNOWLEDGEMENTS

The author would like to sincerely grateful to my advisor, Associate Professor Anongnat Somwangthanaroj, for her invaluable guidance, support, and encouragement through both in research and writing thesis on this master degree program.

The author would also be thankful to Dr. Jitti Kasemchainan as a co-advisor and Associated Professor Soorathep Kheawhom for instruction about my research practice and inspiring my interest that I should do for the better experiments as well as editing this thesis proposal.

The author would like to extend my grateful thanks to Dr. Chutimon Satirapipathkul and Assistant Professor Pornchai Bumroongsri as the chairman and external examiner of this thesis, who provided suggestions and recommendations for this research.

Additionally, the author would like to extend my thanks to all members of Associated Professor Soorathep Kheawhom's group Laboratory and Polymer Engineering Laboratory of the Department of Chemical Engineering, Faculty of Engineering, Chulalongkorn University, for their assistance, discussion, and friendly encouragement in solving problems. Especially, Mr. Wathanyu Kaoian and Miss. Nappaphan Kunanusont.

Finally, my deepest regard is cordially extended to my family and parents, who have always been supporting, loving, understanding as well as encouragement during my master degree study.

จุฬาลงกรณ์มหาวิทยาลัย
CHULALONGKORN UNIVERSITY

Jirapha Pimoei

TABLE OF CONTENTS

	Page
.....	iii
ABSTRACT (THAI)	iii
.....	iv
ABSTRACT (ENGLISH).....	iv
ACKNOWLEDGEMENTS.....	v
TABLE OF CONTENTS	vi
LIST OF TABLES	ix
LIST OF FIGURES	x
Chapter I Introduction.....	1
1.1 Background	1
1.2 Objective	2
1.3 Scope of research	2
1.4 Research plan	3
Chapter II Theory and Literature review.....	4
2.1 Zinc-iodine batteries	4
2.1.1 Overview	4
2.1.2 Zinc electrode	5
2.1.3 Electrolyte.....	5
2.1.4 Separator	5
2.1.5 Iodine electrode	6
2.2 Binder for electrode	7

2.2.1 Polyvinyl alcohol (PVA)	7
2.2.2 Sodium carboxymethyl cellulose (Na-CMC)	8
2.2.3 Sodium alginate (Na-Alg)	8
2.2.4 Sodium polystyrene sulfonate (Na-PSS).....	9
2.3 Analytical Techniques	10
2.3.1 Scanning Electron microscope (SEM)	10
2.3.2 Van der Pauw method	10
2.3.3 Iodide precipitation titrations	11
2.3.4 Galvanostatic charge-discharge Test.....	11
2.3.5 Cyclic Voltammetry (CV).....	12
2.3.6 Electrochemical Impedance Spectroscopy (EIS).....	13
Chapter III Experiments.....	16
3.1 Materials.....	16
3.2 Preparation of CR2025 battery type	16
3.2.1 Negative electrode	16
3.2.2 Electrolyte preparation and separator preparation	16
3.2.3 Positive electrode preparation	16
3.2.4 Battery Assembly	17
3.3 Preparation of pouch cell type	17
3.3.1 Negative electrode	17
3.3.2 Electrolyte preparation and separator preparation	17
3.3.3 Positive electrode preparation	18
3.3.4 Battery Assembly	18
3.4 Physical characterizations.....	18

3.4.1 Electrolyte uptake	18
3.4.2 Scanning Electron microscope (SEM)	19
3.4.3 Van der Pauw method	19
3.4.4 Iodide titration	19
3.5 Electrochemical measurements.....	20
3.5.1 Rate capability and cycling capability	20
3.5.2 Self-discharge	20
3.5.3 Cyclic Voltammetry (CV)	20
3.5.4 Electrochemical Impedance Spectroscopy (EIS).....	20
3.5.5 Cycle test of pouch cells.....	21
Chapter IV Results and Discussions.....	22
4.1 Physical properties of electrodes	22
4.2 Electrochemical performance of batteries	25
Chapter V Conclusion.....	36
Appendix Experiments	38
Van de Pauw method	38
Iodide precipitation titrations.....	40
Electrolyte uptake.....	41
REFERENCES	42
VITA	46

LIST OF TABLES

	Page
Table 1 Research plan.....	3
Table 2 Circuit elements used in models.....	15
Table 3 Electrolyte uptake of binder film	22



LIST OF FIGURES

	Page
Figure 1 The basic components and operation of a zinc-iodine cell	4
Figure 2 The schematic diagram of a positive composite electrode.....	6
Figure 3 Molecular structure of polyvinyl alcohol	7
Figure 4 Molecular structure of sodium carboxymethyl cellulose	8
Figure 5 Molecular structure of sodium alginate	9
Figure 6 Molecular structure of sodium polystyrene sulfonate	10
Figure 7 Circular shape sample with four contacts	11
Figure 8 Example of Cyclicvoltammogram [27]	13
Figure 9 Example of Nyquist plots and Equivalent Circuits	14
Figure 10 The relation between Nyquist and Bode plots (right image)	15
Figure 11 The components of a CR2025 battery test cell.....	17
Figure 12 The components of a pouch cell	18
Figure 13 The Van der Pauw method equipment.....	19
Figure 14 image of binder films after a soak in the electrolyte (ZnSO_4 2M) for 24 hr.....	22
Figure 15 An image of a positive electrode processed with a PVA binder.....	23
Figure 16 SEM image of positive electrode processed with (a) PVA, (b) PVA-NaCMC, (c) PVA-NaAlg, and (d) PVA-NaPSS binder.	24
Figure 17 Electronic conductivity of the positive electrode processed with different binders.	24
Figure 18 Cycle performance of zinc-iodine batteries with different binders at current rate 3C. .	26
Figure 19 (a) Rate capability, (b) Discharge specific capacity retention as a function of the current rate (1C, 2C, 3C, 4C, and 6C) for batteries with different binders.	27

Figure 20 Charge and discharge potential profiles of (a) PVA, (b) PVA-NaCMC, (c) PVA-NaAlg, and (d) PVA-NaPSS positive electrodes at different current rates (1C, 2C, 3C, 4C, and 6C).....	28
Figure 21 Self-discharge of batteries with different binders at various times rest in charge state.....	29
Figure 22 Cyclic voltammograms of the zinc-iodine batteries with positive electrode processed with different binders at a scan rate of 5 mV/s	29
Figure 23 Nyquist plots of the positive electrode with (a) PVA, (b) PVA-NaCMC, (c) PVA-NaAlg, (d) PVA-NaPSS binders (at various charge/discharge state), (e) Nyquist plot comparing of fresh batteries and after 1000 cycles	31
Figure 24 Bode plots of the positive electrode with (a,b) PVA, (c,d) PVA-NaCMC, (e,f) PVA-NaAlg, (g,h) PVA-NaPSS binders (at various charge/discharge state).....	32
Figure 25 SEM image of positive electrode processed with PVA, PVA-NaCMC, PVA-NaAlg, and PVA-NaPSS binders (a, b, c, d) before the cycling test, (e, f, g, h) after 100 cycles	33
Figure 26 (a) pouch cell of the zinc-iodine batteries with positive electrode processed with different binders, (b) Electrolytes solution from pouch cell after charge/discharge ten cycles, (c) Iodide concentration diagram from titration of electrolyte.....	34

Chapter I

Introduction

1.1 Background

The use of fossil-based energy, such as coal, petroleum, and natural gas, has released a large amount of greenhouse gas, which causes global warming phenomena. Hence people are turning to alternative energies such as wind, hydro-power, solar power, and biomass, that are renewable and environmentally friendly. Almost all the mentioned clean energies still have a common challenge of inconsistency in power generation and supply. For instance, the solar power by the photovoltaic panel is available only in the presence of the sunlight. To ensure continuous delivery of electricity, energy storage systems (ESS) have been introduced [1]. One of the most well-known energy storage systems is a group of batteries; lithium-ion batteries are widely used at the present time. Lithium-ion batteries can provide high energy density and high cyclability. However, these batteries still have some limiting factors, such as environmental concerns and high costs [2]. By contrast, zinc-based batteries are among the most promising alternatives due to various advantages of high theoretical capacity (840 mAh g^{-1}) of metallic zinc, balanced kinetics, and stability in aqueous solutions. Moreover, zinc metal and its compounds are highly abundant in resources, low cost, and acceptable in safety [3].

There are several types of zinc-based batteries, such as zinc-ion and zinc-air, which have been developed so far for better performance compare to those in the past. However, these batteries have limited cycle life as zinc exhibits limited long-term reversibility in aqueous electrolytes. Recently, zinc-iodine batteries have been introduced and demonstrated with an improved cycling performance because of the fast-redox reaction [4]. That iodine has a high redox potential (I^-/I_3^- , 0.536 V vs. SHE) and high theoretical capacity (211 mAh g^{-1}) leads to a promising positive electrode for rechargeable zinc-iodine battery [2].

Rechargeable zinc-iodine batteries mainly comprise zinc metal as a negative electrode, an aqueous electrolyte, a membrane separator, and a positive electrode that contains iodine molecules [5-7]. A zinc-iodine battery was first reported in the 1980s. Still, its development was disrupted by some problems such as lack of suitable iodine carriers, high self-discharge, and zinc dendrite growing during cycling [7]. Tedjar studied on the improvement of the positive electrode

of zinc-iodine batteries using polyvinyl alcohol as a binder and mixed with iodine and carbon powder in a solution. This work demonstrated the self-discharge of the battery, which precludes its application due to the leakage of iodine species from the positive electrode [8]. Anionic polyelectrolytes can be applied as a supportive binder for the positive electrode to mitigate this issue thanks to their capabilities of suppression of iodine crossing over and transferring of other active species. Due to the chemical nature of the anionic polyelectrolytes, they can attract only cations but not anions.

An anionic polyelectrolyte is a polymer that has anionic functional groups regularly existing on its chain. Some examples of these polyelectrolytes are sodium carboxymethyl cellulose (Na-CMC), sodium alginate (Na-Alg), and sodium polystyrene sulfonate (Na-PSS). For zinc-iodine batteries, there have not yet been any reports on the preparation of their positive electrode by using these anionic polyelectrolytes as a supportive binder. As a starting point, the outcomes from the study of these anionic polyelectrolytes for lithium-based batteries would be applied to the zinc-based systems.

Na-CMC was used as a binder for the cathode of lithium-based batteries. The results showed that the Na-CMC binder could improve the electrochemical performance of these batteries. Moreover, it is environmentally friendly and low processing-cost [9, 10]. Na-Alg and Na-PSS were used as a binder for the cathode of lithium-sulfur batteries. The results showed that these binders could make the sulfur cathode exhibited better cycle stability [10-12].

In this study, the anionic polyelectrolyte, including sodium carboxymethyl cellulose (Na-CMC), sodium alginate (Na-Alg), and sodium polystyrene sulfonate (Na-PSS), were investigated as a supportive binder for the positive electrodes in rechargeable zinc-iodine batteries.

1.2 Objective

- 1) To encapsulate iodine using anionic polyelectrolyte in rechargeable zinc-iodine batteries.
- 2) To study the effect of different types of anionic polyelectrolytes on the performance of the rechargeable zinc-iodine battery.

1.3 Scope of research

- 1) Zinc foil was used for the negative electrode.

Chapter II

Theory and Literature review

2.1 Zinc-iodine batteries

2.1.1 Overview

The principle of the batteries is converted chemical energy into electrical energy by transfer of electrons from anode to cathode. The zinc-iodine battery was first reported in the 1980s [2]. Zinc-iodine batteries are composed of anode, separator, cathode, and electrolyte that are illustrated in Figure 1. These are the crucial things to make a functional battery that converts chemical energy into electrical energy [1].

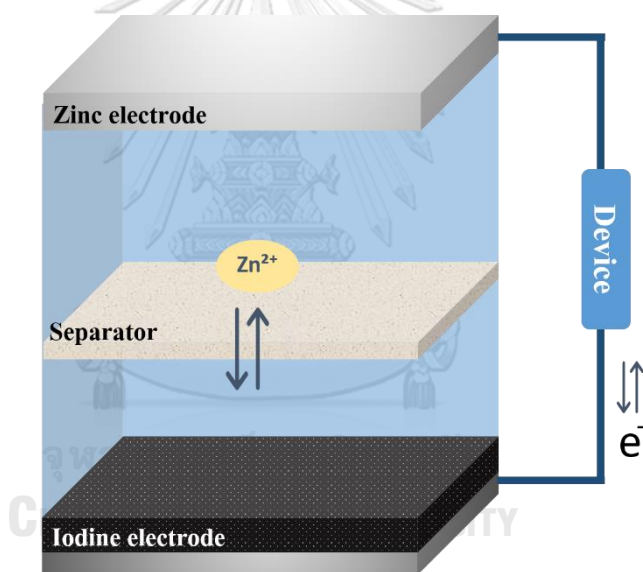


Figure 1 The basic components and operation of a zinc-iodine cell

During the discharging processes, the negative electrode releases electrons to the external device circuit, it is called an oxidation reaction, which is shown in equation 2.1. While the positive electrode accepts electrons from the external device circuit, it is called a reduction reaction, which is shown in equation 2.2. In contrast, during the charging processes, the reaction was reversed at the same electrode. The separator protects electrode contact, avoiding short-circuit. The electrolyte is a medium that contains mobile ions, with cations and anions. A complete circuit produces current and energy.

Negative electrode reaction: $Zn \leftrightarrow Zn^{2+} + 2e^-$ ($\Delta E^0 = -0.76$ V. vs. SHE) (eq. 2.1)

Positive electrode reaction: $I_2 + 2e^- \leftrightarrow 2I^-$ ($\Delta E^0 = 0.536$ V. vs. SHE) (eq. 2.2)

Overall reaction: $Zn + I_2 \leftrightarrow ZnI_2$ ($\Delta E = 1.296$ V.) (eq. 2.3)

2.1.2 Zinc electrode

The Zinc electrode has the advantages for batteries include its abundance, environmental friendliness, low cost, low oxidation and reduction potential, high theoretical capacity (840 mAh g^{-1}), and good reversibility in aqueous electrolyte [3]. Under the acidic condition, zinc has high solubility and become to Zn^{2+} ions. Under mild acid, the dissolution becomes slower because of the high overpotential and lower corrosion activity than a strong acid solution, under a slightly alkaline solution ($8.0 < \text{pH} < 10.5$), the dissolution of Zn will decrease. The main reaction of the zinc electrode in acid and neutral solution can occur as $Zn \leftrightarrow Zn^{2+} + 2e^-$. In general zinc-iodine batteries have used a zinc plate as a negative electrode [2, 4-7, 13-16].

2.1.3 Electrolyte

An electrolyte is a medium for ion movement in batteries, that consist of cation and anion. For zinc-based batteries, Electrolytes are like a zinc-ion source for the zinc intercalation at the positive electrode and zinc deposition at the negative electrode. Normally, rechargeable zinc-based batteries operate in a mildly acid electrolyte and alkaline electrolyte (KOH or NaOH) [3]. However, the important problem with alkaline electrolytes is the high dissolution and corrosion of the zinc electrode. Therefore, aqueous neutral or mildly acidic electrolyte reduces zinc dendrite formation, which leads to high Coulombic efficiency and decreases the corrosion to the zinc electrode that achieves long-term cycling stability. Moreover, such a process is high safety, low cost, and high ionic conductivity. For rechargeable zinc-iodine batteries, zinc sulfate ($ZnSO_4$) has recently been used as the aqueous electrolyte [2, 4, 14].

2.1.4 Separator

The separator has important roles in suppressing electrical contact between positive and negative electrodes while allowing some ion transfer to neutralize charge in the battery. From earlier studies, the cation exchange membrane, such as Nafion, is used for separator in rechargeable zinc-iodine batteries [2, 6, 7, 14, 15]. However, Nafion is too expensive. Xie et al. studied the self-healing of zinc-iodine flow battery by using KI and $ZnBr_2$ as electrolytes

combined with a low-cost polyolefin porous membrane. As a result, a very high-power density and high-performance flow batteries can be achieved [8]. Nevertheless, zinc-iodine batteries without the cation exchange membrane, or with filter paper as a separator have been studied, which is a case that iodine does not certainly pass through the positive electrode [4, 16].

2.1.5 Iodine electrode

Recently, there were studies regarding the use of nanoporous carbon as a positive electrode. Lee et al. reported a hybrid energy storage system employing zinc iodide (ZnI_2) redox electrolyte with nanoporous activated carbon fiber (ACF) cathode and zinc disk anode [11]. Lu et al. designed three-dimensional (3D) graphene foams co-doped with sulfur and nitrogen via an in-situ reduction of graphene oxide and subsequent thermal annealing process [2]. However, the temperature of annealing is so high and expensive, and these studies were zinc-iodine redox flow batteries.

A few earlier studies of the positive electrode of zinc-iodine batteries have been using polymer such as nylon-6, polyvinyl acetate, and polyvinyl alcohol mixing with iodine and carbon powder in a solution, spreading the mixture uniformly on a carbon fiber plate and evaporation of the solvent. These polymers can improve the conductivity performance [7, 8]. The schematic diagram of a positive electrode with a binder, as shown in Figure 2.

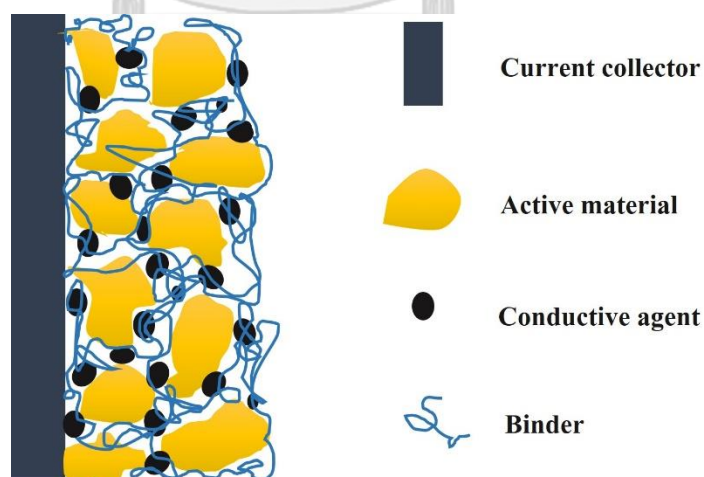


Figure 2 The schematic diagram of a positive composite electrode

2.2 Binder for electrode

Regarding to the above paragraph in which polymer was chosen to use as a binder for the positive electrode of zinc-iodine batteries. Polyvinyl alcohol was chosen to be a binder in this research due to the advantage of combining properties such as good mechanical parameters, easy processing, and low volatility [8].

2.2.1 Polyvinyl alcohol (PVA)

Poly (vinyl alcohol) (PVA) is a semi-crystalline and water-soluble polymer, which has been explored extensively because of its many interesting physical properties such as high flexibility and tensile strength, high dielectric strength (1000kV/mm), good charge storage capacity, dopant dependent electrical properties that arise from the presence of OH groups and the hydrogen bond formation [17]. Moreover, it is also non-toxic and susceptible to ultimate biodegradation in the presence of suitably acclimated microorganisms [18]. The molecular structure of PVA is shown in Figure 3.

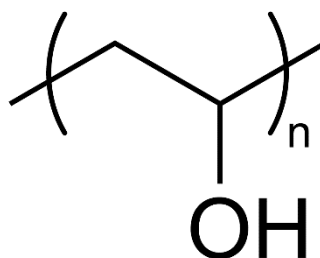


Figure 3 Molecular structure of polyvinyl alcohol

However, there are some problems when using polyvinyl alcohol as a binder of the positive electrode of zinc-iodine batteries with self-discharging because I_3^- ion could leak from the positive electrode and transport to the negative electrode [8]. To fix this problem, supportive binders such as anionic polyelectrolyte will be observed. The natural chemistry of anionic polyelectrolyte can attract the only cation and distract anion. Thus, it will be a good cation exchange material which allows Zn^{2+} transfer from the negative to the positive electrode while suppressing the I_3^- and I^- transfer from the positive electrode.

The present study will show that using a binder as a PVA blend with anionic polyelectrolytes such as sodium carboxymethyl cellulose, sodium alginate, and sodium

polystyrene sulfonate can make the iodine electrode. Moreover, this electrode will be better in electrochemical performance.

2.2.2 Sodium carboxymethyl cellulose (Na-CMC)

Sodium carboxymethyl cellulose (Na-CMC), a water-soluble binder, is an anionic polyelectrolyte with dissociation to form carboxylate anionic functional groups. It is a chemical derivative of cellulose where some of the hydroxyl groups (-OH) are substituted with carboxymethyl groups (-CH₂COOH) [9, 10]. The molecular structure of Na-CMC is shown in Figure 4. It is frequently used in research reports but has not been successfully implemented in electrodes alone in manufacture because of its brittle characteristic [19].

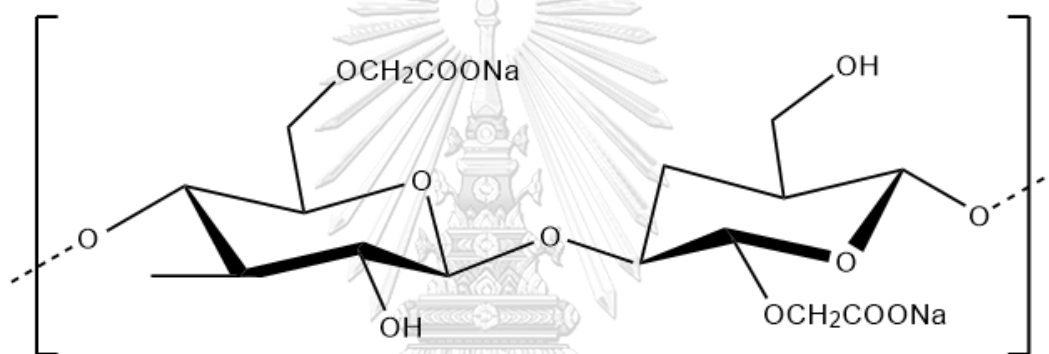


Figure 4 Molecular structure of sodium carboxymethyl cellulose

Wang et al. used Na-CMC as a binder for the LMNO cathode of lithium-ion batteries compared with conventional binders [9]. In the same way, Condi group used Na-CMC as a binder for the cathode of lithium-sulfur batteries [10]. The results show that the Na-CMC binder could improve the electrochemical performance of these batteries. Moreover, it is also environmentally friendly and low processing costs [9, 10].

2.2.3 Sodium alginate (Na-Alg)

Sodium alginate (Na-Alg) is produced from brown seaweed using dilute alkali. It mainly consists of the sodium salt of alginic acid, and a polysaccharide composes of 1–4-linked β -D-mannuronic acid (M) and α -L-guluronic acid (G) [10], whose structure resembles that of Na-CMC. The molecular structure of Na-Alg is shown in Figure 5. Bao et al. demonstrated the use of

Na-Alg as the binder for the cathode of lithium-sulfur batteries, which displayed charge-discharge capacity and the capacity retention rate of Na-Alg sulfur cathode was 508 mAh g^{-1} and 65.4% at the 50th cycle with a current density of 335 mA g^{-1} [11]. Same as the Na-CMC, Condi group used Na-Alg as a binder for the cathode of lithium-sulfur batteries. The results show that the Na-Alg binder could improve the electrochemical performance of these batteries by maintained 608 mAh g^{-1} during a test 100 cycles when discharge voltage was limited to 1.8 V [10].

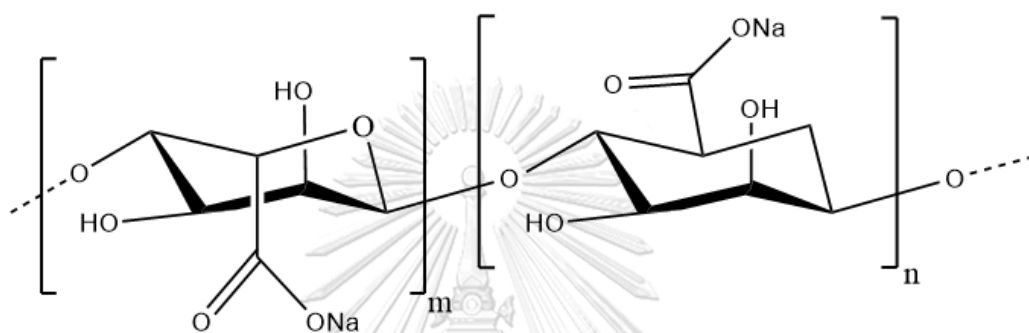


Figure 5 Molecular structure of sodium alginate

2.2.4 Sodium polystyrene sulfonate (Na-PSS)

Sodium polystyrene sulfonate (Na-PSS) is widely used for the treatment of hyperkalemia. It is a synthetic cation-bound resin that can exchange sodium cations for potassium in the gastrointestinal (GI) lumen, resulting in increased fecal potassium excretion that leads to decreased serum potassium levels [20]. Yang et al. used Na-PSS as a component of a polyelectrolyte binder for a sulfur electrode in lithium-sulfur batteries. This results, the capacity and cycle performance of the battery was improved evidently when the cell discharged to 1.8V because the sulfonate group has good assisting Li^+ ion transportation [12]. Moreover, the study of compatibility between PVA and NaPSS has been reported [21]. The molecular structure of Na-PSS is shown in Figure 6.

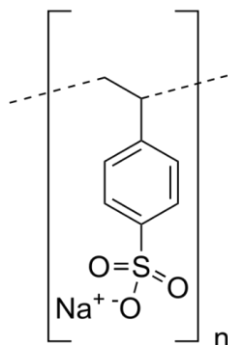


Figure 6 Molecular structure of sodium polystyrene sulfonate

2.3 Analytical Techniques

Several characterization techniques were applied to battery researches. These were not only used for characterizing the battery cells, but also for determining the cell parameters. The power-energy, the cycling behavior, the charge transfers characteristic change upon the cycling, the phase transformation of the host materials, and the electrode-electrolyte interphase can be investigated via the following techniques.

2.3.1 Scanning Electron microscope (SEM)

The scanning electron microscope (SEM) is a traditional characterization technique for studying electrode microstructure to observe their morphology and distribution of particles.

2.3.2 Van der Pauw method

The Van der Pauw measurement is a technique to measure specific resistivity and electrical conductivity accurately. For measuring the resistivity of a circular shaped sample in a dual configuration, as shown in Fig. 7, gives equation (2.4)

$$\text{Resistivity } (\rho) = \frac{\pi d}{\ln 2} \left(\frac{R_{12,43} + R_{23,14}}{2} \right) F(Q) \quad (2.4)$$

With $F(Q)$ is found by solving the equation:

$$\frac{Q-1}{Q+1} = \frac{F}{\ln 2} \cosh^{-1} \left(\frac{e^{\left(\frac{\ln 2}{F}\right)}}{2} \right) \quad (2.5)$$

When $R_{12,43} > R_{23,14}$

$$Q = \frac{R_{12,43}}{R_{23,14}} \quad (2.6)$$

To determine the resistance value, the current must be varied to record the obtained voltage. The resistivity is then calculated following equation 2.4 [22-24].

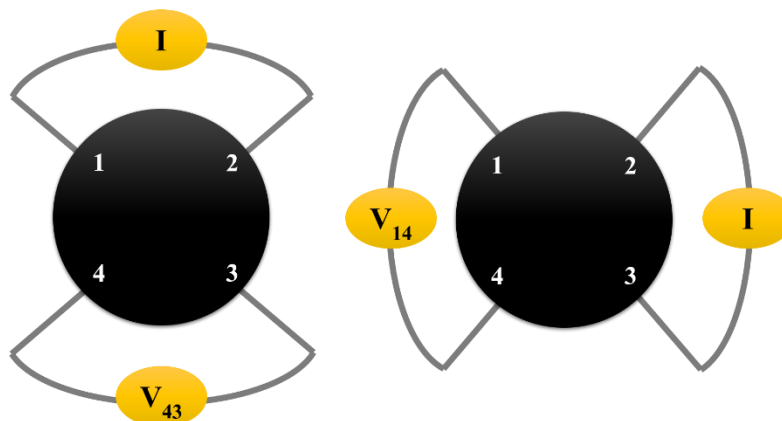
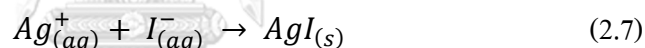


Figure 7 Circular shape sample with four contacts

2.3.3 Iodide precipitation titrations

The most important precipitation processes in titrimetric analysis utilize silver nitrate (AgNO_3) as the reagent (argentometric processes). This technique is commonly used to determine the quantity of halide groups (fluoride, chloride, bromide, and iodide). The precipitates are the insoluble silver halide, in this study mainly considered the silver iodide (AgI) with the yellow precipitate. The reaction of silver iodide shows as equation (2.7).



During the titration, the endpoints are hard to notice. Therefore, a suitable indicator must be used. Eosin (tetrabromofluorescein) is an indicator, which is widely used for silver iodide precipitation titration. Eosin is a strong acid with being used down to a pH of 1-2—the color change from yellowish to magenta at the endpoint [25, 26].

2.3.4 Galvanostatic charge-discharge Test

The standard method for determination of the cell performance and cyclability is the applied throughput of discharge and charge current to the cell repeatedly within reached the set specific voltage. The result is the voltage profile with respect to time. The obtained results can be used to determine the charge/discharge specific capacity, energy density, and Coulombic efficiency. Moreover, the rate capability by varied current rates as a function of cycle number can be observed. In general, the testing current was normalized with the amount of the active host material that the electrode contained, as shown in equation (2.8). [27]

$$\text{Current Density} = \frac{I}{m_{ac}} \quad (2.8)$$

The capacity of the positive electrode is determined by measuring the total charge. That is delivered from the positive electrode upon the charging or discharging. Specific capacity could be obtained via the integration of the current with respect to the time from the initial state to the cut-off state, then normalize this value by the mass of the active material (m_{ac}), as shown in equation (2.9).

$$\text{Specific Capacity} = \frac{1}{m_{ac}} \left(\int_{t_0}^{t_f} Idt \right) \quad (2.9)$$

The energy for the charging and energy obtained from the discharging process can be calculated by

$$\text{Energy Density} = \frac{1}{m_{ac}} \left(\int_{t_0}^{t_f} IVdt \right) \quad (2.10)$$

The percentage of discharging capacity compared with the charging capacity, called Coulombic efficiency, is one of the most critical factors to consider the reversibility of the battery. This value can be calculated by using

$$\text{Coulombic Efficiency} = \frac{\text{Discharge Capacity}}{\text{Charging Capacity}} \times 100\% \quad (2.11)$$

2.3.5 Cyclic Voltammetry (CV)

The technique to investigate the redox reaction characteristic of the electrode is cyclic voltammetry. The potential of the working electrode, with respect to the reference electrode, was linearly started from an initial point to the vertex point, then ramped in the opposite direction to the final point. The output from this action is the rate of the redox reaction in the form of current density vs. voltage: cyclic voltammogram. Figure 8 shows a reduction peak, which is more positive in potential values, and then reverse directions to more negative potentials, indicate oxidation reaction peak [27].

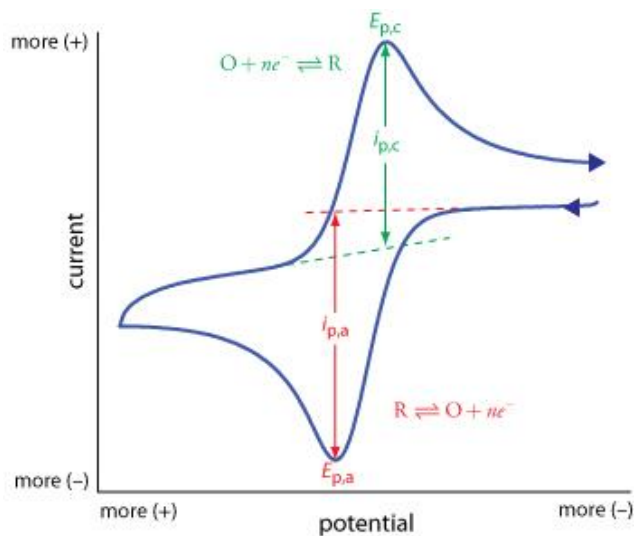


Figure 8 Example of Cyclicvoltammogram [27]

2.3.6 Electrochemical Impedance Spectroscopy (EIS)

The electrochemical impedance spectroscopy is the technique for analysis of the elementary reaction step of the electrochemical reaction and analyzed circuit parameters, such as internal resistance (R), polarization resistance (R_p), charge transfer resistance (R_{ct}), double-layer capacitance (C_{dl}), and Warburg impedance (Z_w). Applying both frequency-dependence sinusoidal potential and static potential was tested the cell. The result of this technique is the impedance spectra or Nyquist plot, which comprise the real impedance (Z_{re}) and imagine impedance (Z_{im}) at each frequency, as shown in Fig. 9. Moreover, the relation between the Nyquist plot and Bode plots is shown in Figure 10. Bode plot is an absolute impedance and phase angle of impedance as a function of frequency.

The equivalent circuits and circuit elements are shown in Figure 9 and Table 2. Internal resistance, which widely refers to electrolyte resistance or solution resistance (R_s), is often a factor in the impedance of an electrochemical cell. The solution resistance value depends on the temperature, ionic concentration, type of ions, and the geometry of the area, in which the current is carried. Double-layer capacitance (C_{ld}) is capacitance at electrode surface contact with an electrolyte solution. This double layer is formed ions from the electrolyte solution to attach active material ion in the electrode surface. The double-layer capacitance value depends on many variables such as electrode potential, ionic concentrations, temperature, types of ions, and

electrode roughness. The double-layer capacitance value depends on many variables, such as electrode potential, ionic concentrations, temperature, types of ions, electrode roughness, etc. are all factors. Polarization Resistance (R_p) is the potential of an electrode forced away from its value at open-circuit. When an electrode is polarized, cause current flows through electrochemical reactions, which occurs at the electrode surface. The current content is controlled by the diffusion of reactants and the kinetics of the reactions. A single kinetically controlled electrochemical reaction forms charge transfer resistance (R_{ct}). Considering when to contact a metal substrate in an electrolyte, this metal can electrolytically dissolve into the electrolyte; according to the forward reaction, electrons can enter the metal, and metal ions can diffuse into the electrolyte. Therefore, the charge is being transferred. This charge transfer reaction has a certain speed, where the speed depends on the kind of reaction, the concentration of the reaction products, the temperature, and the potential. Warburg-impedance (Z_w) can indicate the diffusion of ion in a bulk solid electrode. The impedance depends on the frequency. At high frequencies, the Warburg impedance is small due to the short distance of diffusing reactants. While, at low frequencies, the reactants have to diffuse farther, increasing the Warburg impedance. From the Nyquist Plot, the Warburg impedance displays a diagonal line with a slope of 45° [28-31].

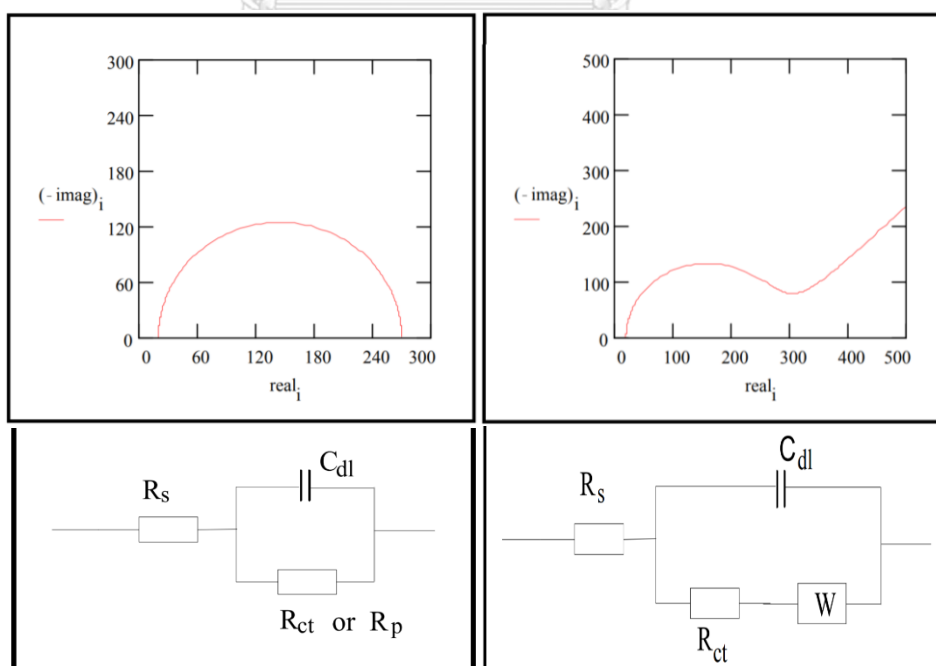


Figure 9 Example of Nyquist plots and Equivalent Circuits

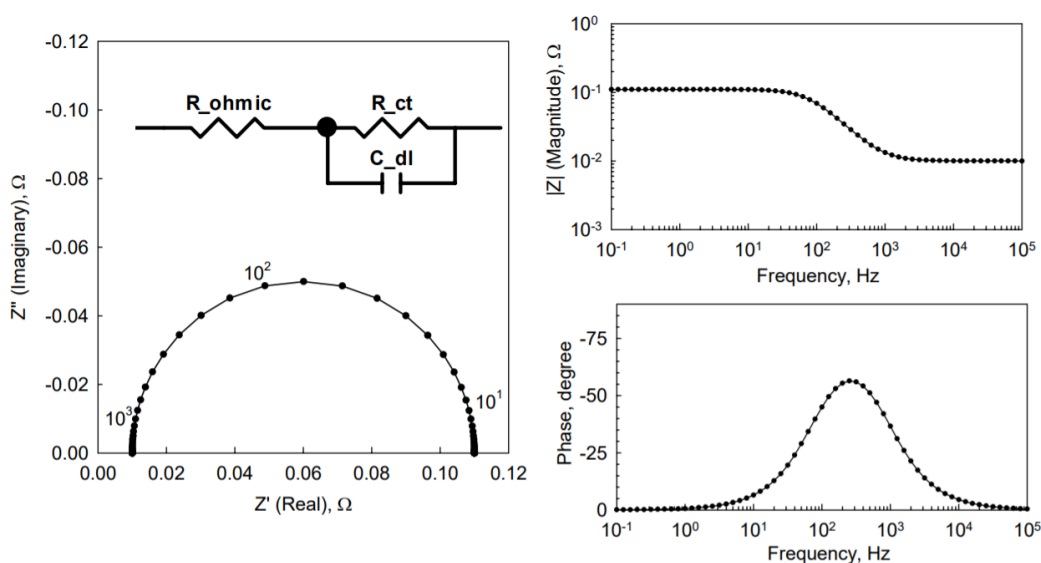


Figure 10 The relation between Nyquist and Bode plots (right image)

In battery application, this technique is a powerful tool to interpret the change in charge transfer characteristic upon cycling. The impedance spectra were fitted with some proposed model in order to retrieve the internal resistance, the double-layer capacitance, the charge transfer resistance, and other associate parameters to the charge transport in the battery. Almost all of the model for the impedance analysis is the network of basic electrical components, for instance, resistor, capacitor, and inductor.

CHULALONGKORN UNIVERSITY

Table 2 Circuit elements used in models

Equivalent Element	Impedance
R	R
C	$1/j\omega C$
L	$j\omega L$
W (infinite Warburg)	$1/Y_0\sqrt{(j\omega)}$
O (finite Warburg)	$\text{Tanh}(B\sqrt{(j\omega)})/Y_0\sqrt{(j\omega)}$
Q (CPE)	$1/Y_0(j\omega)^\alpha$

Chapter III

Experiments

3.1 Materials

Iodine crystal with 99.8% purity was supplied by Kemaus. Potassium iodide (KI, 99.0%) was supplied by Univar. Charcoal activated powder technical grade was purchased from PanReac plupliChem. Supper carbon (supper P, Timcal) and polyvinyl alcohol (PVA) (MW. 100,000) were purchased from Chem-supply. Sodium carboxymethyl cellulose (Na-CMC) (medium viscosity, MW. 90,000) was purchased from Sigma-Aldrich. Sodium alginate (Na-Alg) (food grade) was purchased from Loba Chemie, and sodium polystyrene sulfonate powder (Na-PSS) (MW. 1,000,000) was purchased from Sigma-Aldrich. Graphite foil (Thickness: 0.05 mm and 0.10 mm), glass microfiber paper (GF/C, 1.2 μm), and zinc sulfate 7-hydrate ($\text{ZnSO}_4 \cdot 7\text{H}_2\text{O}$) (AR grade, MW 287.58 g/mol) was purchased from Kemaus. Zinc foil (Thickness: 0.1 mm), and blank coin cell CR2025. Silver nitrate (AgNO_3) and Eosin (tetrabromofluorescein) were purchased from Panreac.

3.2 Preparation of CR2025 battery type

3.2.1 Negative electrode

A zinc foil (thickness: 0.1 mm) was used for a negative electrode for the battery. The zinc foil was cut into a circular shape with 15 mm in diameter.

3.2.2 Electrolyte preparation and separator preparation

ZnSO_4 2 M was used as an electrolyte in batteries. The electrolyte preparation was to dissolve a certain amount of ZnSO_4 into DI water using a magnetic stirrer at room temperature to dissolve well. A separator was a glass microfiber (pore size: 1.2 μm), which was cut into a circular shape with 19 mm in diameter.

3.2.3 Positive electrode preparation

The positive electrodes were prepared from a mixture of iodine, in which the solubility was increased by adding KI. Adsorbed iodine on activated carbon was used as an active material. Super-P was used as a conducting agent. PVA was used as a binder. Anionic polyelectrolyte, such Na-CMC, Na-Alg, and Na-PSS was used as a supportive binder. The weight ratio of active

material: conducting agent: binder was 80:10:10. DI Water was used as a solvent. The mixture should be stirred by a magnetic stirrer overnight to confirm well-mixing. Then, the resulting substance was coated on the graphite foil by using the doctor blade machine and dried at room temperature to remove the solvent [32]. Finally, the positive electrode sheet was obtained. The sheet was cut to a circular shape with a diameter of 15 mm.

3.2.4 Battery Assembly

The batteries were fabricated as a CR2025 cell that includes the top cap, cone spring, spacer, negative electrode, separator, positive electrode, and bottom cap, respectively, as shown in Fig. 11. During assembled the component, the electrolyte was dropped onto separator around 0.5 mL. Then, the cell was closed with pressure around 1 ton/cm² by a crimping machine.

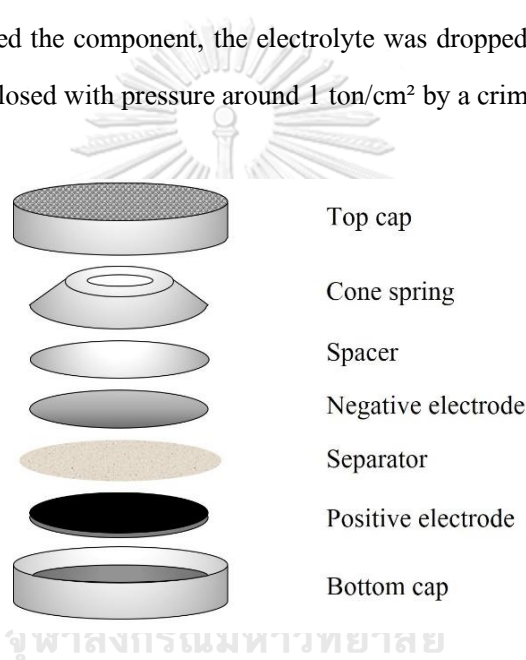


Figure 11 The components of a CR2025 battery test cell

3.3 Preparation of pouch cell type

3.3.1 Negative electrode

A zinc foil (thickness: 0.1 mm) was used for a negative electrode for the battery. The foil was cut into a rectangular shape with 3.5*7.3 cm.

3.3.2 Electrolyte preparation and separator preparation

ZnSO₄ 2 M was used as an electrolyte in batteries, in which the preparation was similar to that for CR2025 cell type. A separator was a glass microfiber (pore size: 1.2 μm), which was cut into a rectangular shape with 4.0*7.5 cm.

3.3.3 Positive electrode preparation

The positive electrode mixtures were prepared in the same way as for CR2025 cell type, but using graphite foil with 0.10 mm thickness as a current collector replacement. The mixture was coated on the graphite foil by using the doctor blade machine and was dried at room temperature to remove the solvent. Finally, the positive electrode sheet was obtained. The sheet was cut to a rectangular shape with 3.8*7.5 cm.

3.3.4 Battery Assembly

The batteries were fabricated as a pouch cell that includes the aluminum laminated film, negative electrode, separator, positive electrode, respectively [33], as shown in Fig. 12. During assembled the component, the electrolyte was used around 15 mL. Then, the cell was closed by a sealer with a temperature of 175 °C.

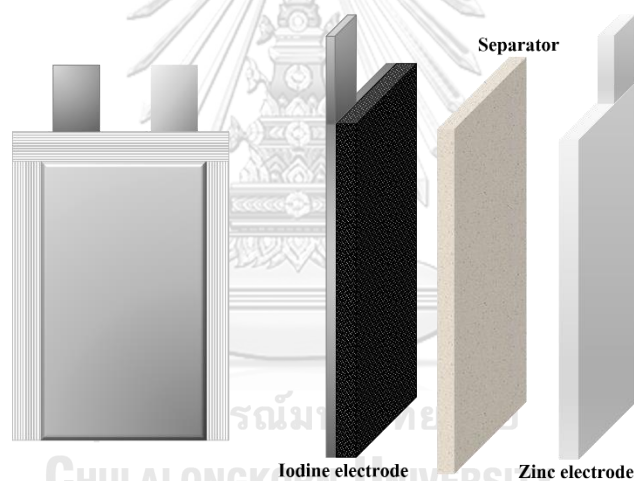


Figure 12 The components of a pouch cell

3.4 Physical characterizations

3.4.1 Electrolyte uptake

Binder films were prepared by solution casting method. They were then cut the film into a circular shape with 15 mm in diameter. The film was weighed before and after soaking in 2M ZnSO₄ for 24 hr. The percent of the increase in film weight was calculated to determine electrolyte uptake value [19, 34, 35].

3.4.2 Scanning Electron microscope (SEM)

The SEM instrument was used to investigate the morphology of the positive electrode, both initial and after cycling. The battery was charged and discharged around 100 cycles at a constant current of 3C. Then the positive electrode was disassembled from the battery and the morphology was observed by SEM.

3.4.3 Van der Pauw method

The specific resistivity of positive electrodes was measured from the Van der Pauw method. The positive electrode was cut into a circular shape with 15 mm in diameter, it was then tested with the instrument (as shown in Fig 13) by applying various current from 1 to 5 mA, both positive and negative direction. After applied current, the voltage has presented the value was then recorded to calculate the resistivity. The resistivity can be transformed into electrical conductivity by multiply -1.

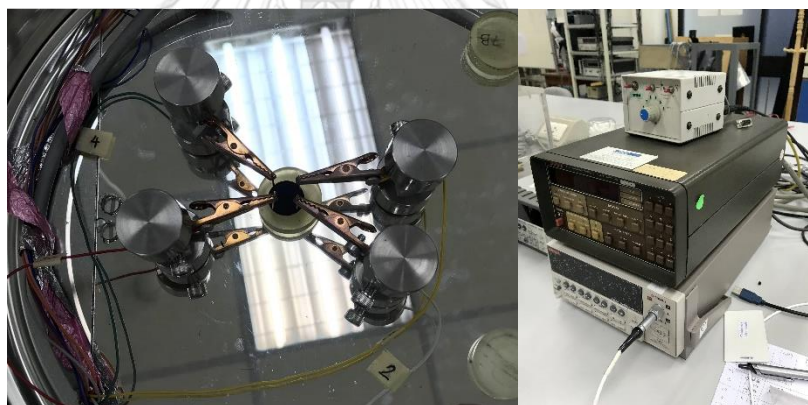


Figure 13 The Van der Pauw method equipment

3.4.4 Iodide titration

The electrolyte was collected from the disassembly of the pouch cell after 10 cycles charge/discharge test. The electrolyte was titrated with silver nitrate (AgNO_3) 0.05M and eosin 0.1%w/v as an indicator if the electrolyte has high iodide content, the use of AgNO_3 would be high too. The obtained result of this test was a diagram of iodide concentration with various binders in positive electrodes.

3.5 Electrochemical measurements

3.5.1 Rate capability and cycling capability

The galvanostatic charge/discharge tests were carried out by using the multi-channel battery tester. To estimate the rate capability, the current needed to be varied stepwise by 1C, 2C, 3C, 4C, and 6C, respectively. The results showed the polarization profile and capacity vs. cycle at different rates with respect to current. To estimate the cycling capability. The current was kept constant at 3C for cycling up to 1000 cycles. The results showed the capacity retention when the battery was charged and discharged; the Coulombic efficiency from this data can be determined. The operating voltage for both schemes is in the potential range of 0.7 to 1.7V.

3.5.2 Self-discharge

The galvanostatic charge/discharge tests were used to estimate the self-discharge by setting time rest at the charge state. The time rest was varied by 0 min, 30 min, 1 hr, 2 hr, 4 hr, 8 hr, one day, two days, three days, one week, and two weeks, respectively. The operating voltage is in the potential range of 0.7 to 1.7V. The obtained result of this test was a diagram between capacity retention and time rest of batteries with different binders.

3.5.3 Cyclic Voltammetry (CV)

VersaSTAT tool was used to analyze the oxidation and reduction behaviors of batteries. The test was in the range of potential at 0.7-1.7 Volts, with a scan rate of 5 mV/s. The characteristics of current vs. the potential were obtained. Each sample can be compared with the others according to the electrochemical behavior.

3.5.4 Electrochemical Impedance Spectroscopy (EIS)

EIS measurements were carried out with VersaSTAT tool VersaStudio software potentiostatic EIS mode in the frequency range between 200 kHz and 10 mHz. The fresh batteries and batteries after charge/discharge test 1000 cycles were evaluated. Including batteries at different charge/discharge states, which were varied by 50%, 100% of charge capacity, and 50%, 100% of discharge capacity, were observed too. The impedance spectra were collected, indicating the electronic and ionic conductivities, as well as differentiating the ionic transfer performance of each binder used in this work.

3.5.5 Cycle test of pouch cells

Pouch cells, whose positive electrodes processed with other binders, were cycle tested by galvanostatic charge/discharge for 10 cycles. The current was fixed at 1 mA/cm^2 while the operating voltage is in the potential range of 0.7 to 1.7V.



Chapter IV

Results and Discussions

4.1 Physical properties of electrodes

The electrolyte uptake property of binder films was evaluated from the weighting of binder films before and after soaking in electrolyte solutions for 24 hr, as shown in Fig 14. The result displays that the percent weight increases after soaking these films in the electrolyte as shown in Table 3. The PVA-NaCMC film has the highest electrolyte uptake value, with 127.38%. While PVA-NaAlg and PVA-NaPSS have medium values of percent electrolyte uptake, with 98.56% and 49.63%, respectively. In contrast, PVA has the lowest value among the four films, with 31.3%, indicating that higher stability in the electrolyte (ZnSO_4 2M) [19, 36]. However, the excellent electrolyte uptake of polymer binder leading to higher ion conductivity.

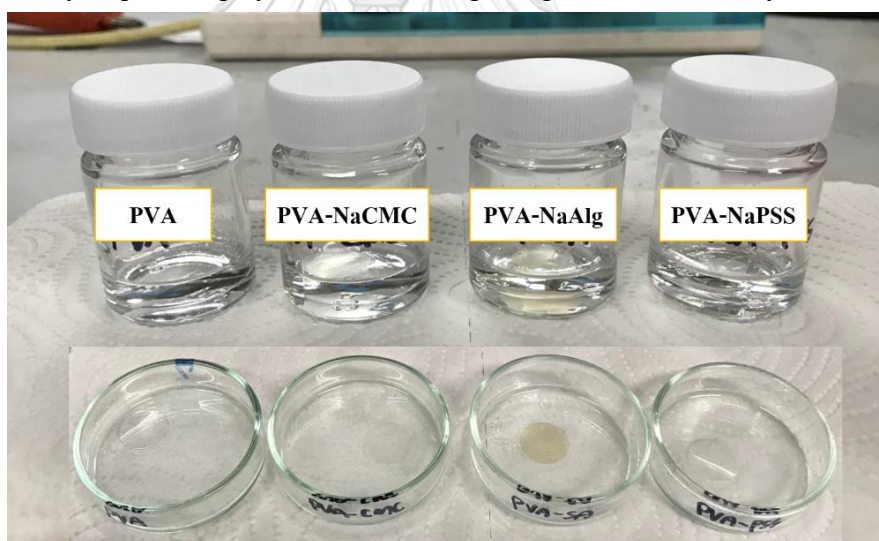


Figure 14 image of binder films after a soak in the electrolyte (ZnSO_4 2M) for 24 hr.

Table 3 Electrolyte uptake of binder film

Type of binder	Electrolyte uptake (%)
PVA	31.3
PVA-NaCMC	127.38
PVA-NaAlg	98.56
PVA-NaPSS	49.63

Figure 15 shows the appearance of the positive electrode processed with PVA binder after preparation with a mixture of active material, conductive agent, and binder, and then coating on graphite foil. The surface of a positive electrode looks relatively smooth and homogeneous. The physical morphology of positive electrodes from SEM in Figure 16 (a-d) shows active material and conductive agent distribution in binder networks. The PVA-NaCMC, PVA-NaAlg, and PVA-NaPSS reveal higher carbon (super-P) content surrounding the active material particle than those positive electrodes, which indicate better electron percolating of these electrodes. For this reason, the electrochemical performance of these batteries much improves.



Figure 15 An image of a positive electrode processed with a PVA binder.

The electronic conductivity of the pristine positive electrode processed with different binders is shown in Fig. 17. The electronic conductivity values are 7297, 7087.9, and 6735.9 S/m of PVA-NaCMC, PVA-NaAlg, and PVA-NaPSS binder, respectively. In comparison, the PVA binder gives 6731.8 S/m of electronic conductivity, which is the lowest value among four-electrode processed with different binders. Since these anionic polyelectrolytes have the distribution of carbon conductive around active material better than a positive electrode using only PVA binder, leading to higher electrical conductivity [19, 37].

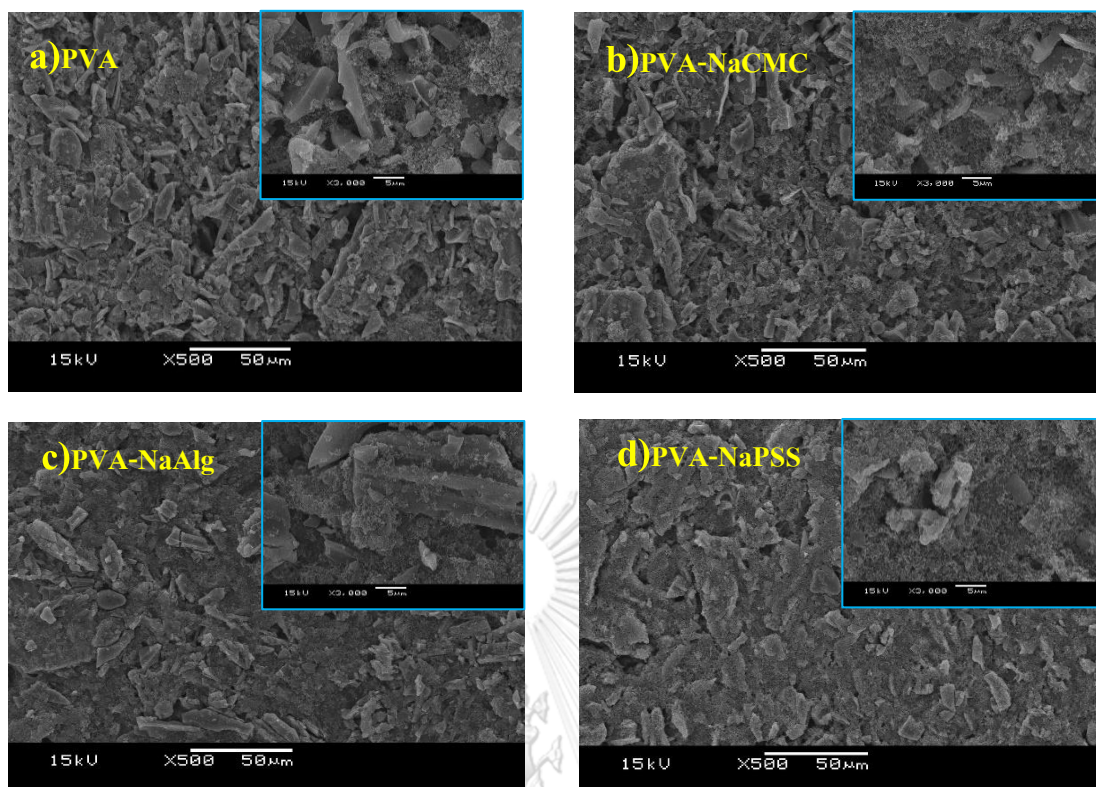


Figure 16 SEM image of positive electrode processed with (a) PVA, (b) PVA-NaCMC, (c) PVA-NaAlg, and (d) PVA-NaPSS binder.

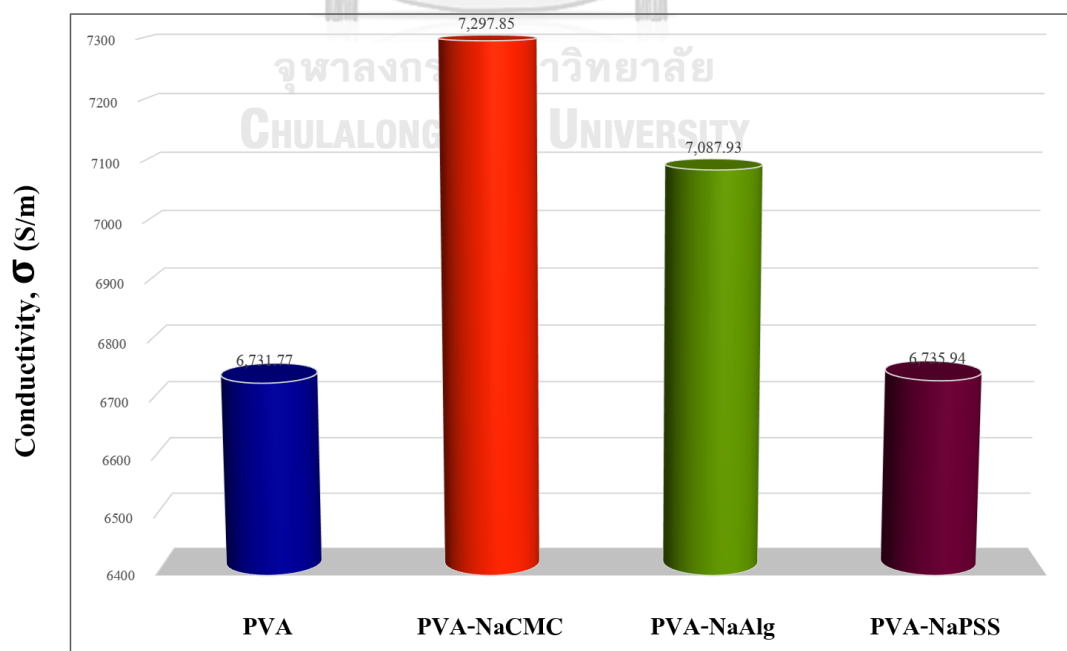


Figure 17 Electronic conductivity of the positive electrode processed with different binders.

4.2 Electrochemical performance of batteries

To investigate the effect of a supportive binder on the positive electrode. The electrochemical performances were studied. The charge/discharge specific capacity of the positive electrodes containing either PVA, PVA-NaCMC, PVA-NaAlg, or PVA-PSS was plotted against cycle number, as shown in Fig. 18. The result demonstrated that the capacities of all positive electrodes decrease gradually with an increase in cycle number. To compare the following performance, the current rate was fixed at 3C. The initial discharge specific capacity of the PVA positive electrode is $104.06 \text{ mAh g}^{-1}$ and remains 94.19 mAh g^{-1} after 1000 cycles. The capacity retention is around 90.5% at the end of cycling. Interestingly, the positive electrode using PVA-NaCMC as a binder has an initial capacity of $127.37 \text{ mAh g}^{-1}$, which is higher than the electrode processed with other binders and remains $116.69 \text{ mAh g}^{-1}$ after 1000 cycles with the capacity retention of 91.6%. While the positive electrode using PVA-NaAlg as a binder has an initial capacity of $114.14 \text{ mAh g}^{-1}$ and remains $102.12 \text{ mAh g}^{-1}$ after 1000 cycles with the capacity retention of 89.5%. The positive electrode using PVA-NaPSS as a binder has an initial capacity of $106.05 \text{ mAh g}^{-1}$. It remains 98.21 mAh g^{-1} after 1000 cycles with the capacity retention of 92.6%, which is higher than those of the electrode processed with other binders. The presence of the anionic polyelectrolytes can improve the specific capacity and cycling capability, especially the electrode with NaCMC and NaPSS as a supportive binder which has the highest specific capacity and the best cycling stability, respectively. The excellent cycle performance could be due to the uniform distribution of active material and conductive agent in PVA-NaCMC and PVA-NaPSS binder matrix.

Figure 19 (a) shows a comparison of the discharge specific capacity at various rates by using different binders. It can be seen that the discharge specific capacity gradually decreases when increasing the current rate from 1C to 6C. A positive electrode with a PVA-NaCMC binder gives higher practical discharge specific capacity than the electrodes processed with the other supportive binders at all rates. While the positive electrode with PVA as a binder provides lowest discharge specific capacity among four electrodes at all rates.

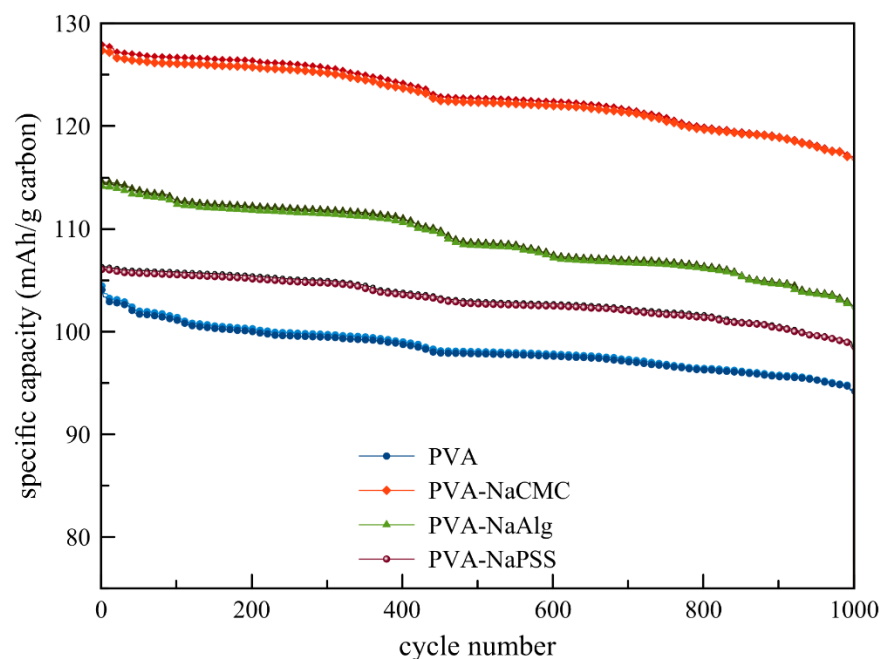


Figure 18 Cycle performance of zinc-iodine batteries with different binders at current rate 3C.

This data was converted to discharge specific capacity retention, as shown in Fig 19 (b). The result presents the same trend as the specific capacity decreases when increasing the current rate following the rate capability. The positive electrodes with PVA, PVA-NaCMC, PVA-NaAlg, and PVA-NaPSS binders give discharge specific capacity retention, at the current rate from 1C to 6C, 81.8%, 83.3%, 81.8%, and 82.8%, respectively. Accordingly, using anionic polyelectrolytes can provide high rate capability.

The charge/discharge potential profiles of the zinc-iodine batteries with different binders at various current rates from 1C to 6C are shown in Fig 20 (a-d). The curves display a typical discharge potential plateau, corresponding to the single-steps of the reduction reaction of iodine during the discharge process at around 1.2 V, which has the same trend with every binder. With the increase of current rates 1C, 2C, 3C, 4C, and 6C, the charge/discharge curves significantly decrease because the limit of zinc ion transportation lead the polarization at the high current rate [38]. However, using anionic polyelectrolytes as supportive binders have smaller polarization than a pure PVA binder, noticed from the charge/discharge potential plateau of the positive

electrodes using these almost overlap in the same line at all current rate. Therefore, anionic polyelectrolytes can improve the rate capability of rechargeable zinc-iodine batteries.

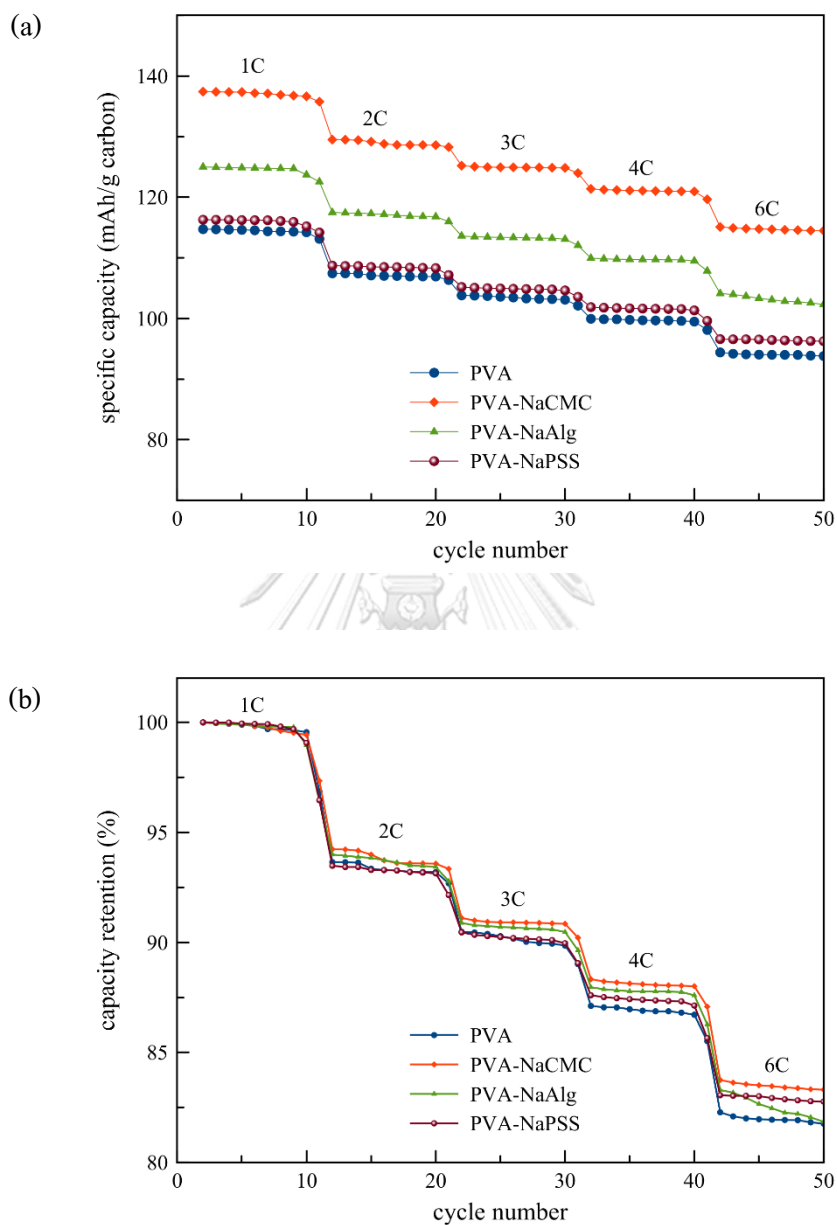


Figure 19 (a) Rate capability, (b) Discharge specific capacity retention as a function of the current rate (1C, 2C, 3C, 4C, and 6C) for batteries with different binders.

To estimate the self-discharge of batteries using different binders, as shown in Fig. 21. The rest time of the batteries was varied at charge state for 30 min, 1 hr, 2 hr, 4 hr, 8 hr, one day, two days, three days, one week, and two weeks. The result shows that PVA-NaAlg binder has the

highest capacity retention, which is 79.3% after being left to rest for two weeks in charge state. In contrast, the PVA binder gives the lowest capacity retention, with 68.9% in the same state. Consequently, anionic polyelectrolytes can reduce the self-discharge effect of rechargeable zinc-iodine batteries.

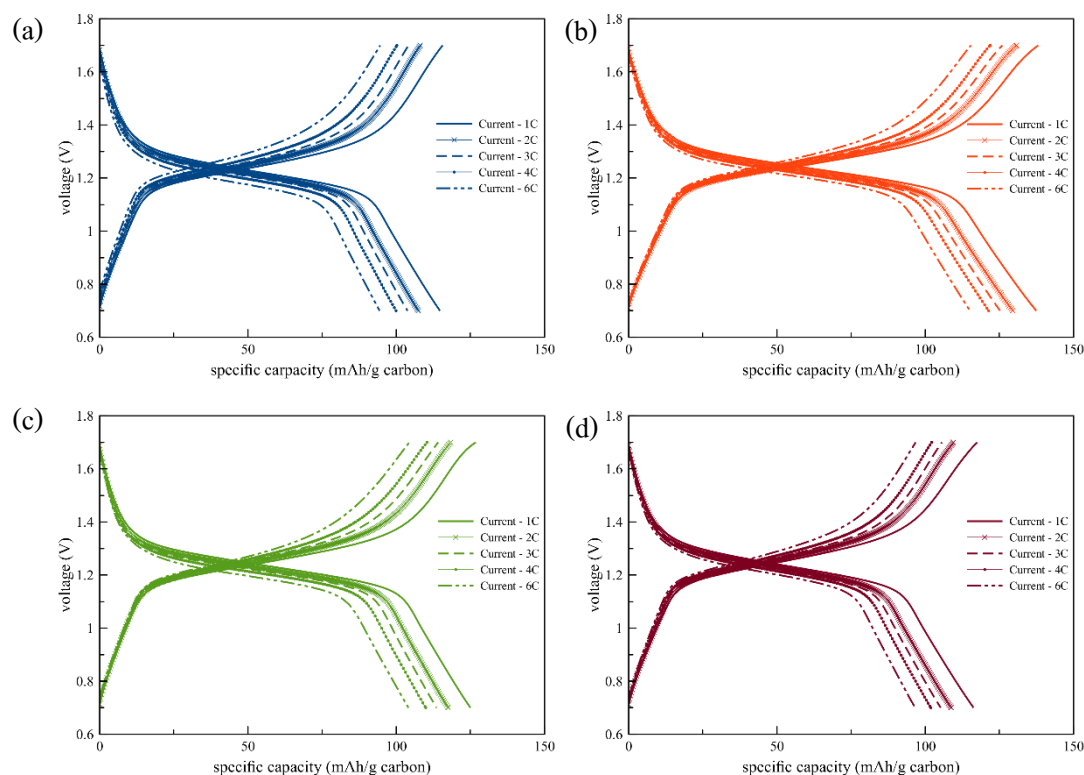


Figure 20 Charge and discharge potential profiles of (a) PVA, (b) PVA-NaCMC, (c) PVA-NaAlg, and (d) PVA-NaPSS positive electrodes at different current rates (1C, 2C, 3C, 4C, and 6C).

To estimate the electrochemical reaction and mechanism that enhance the performance of batteries, the cyclic voltammetry (CV) and electrochemical impedance spectroscopy (EIS) were studied. The cyclic voltammograms of the positive electrodes with different binders at a voltage range of 0.7 - 1.7 V and a scan rate of 5 mV/s are presented in Fig. 22. The CV profiles can identify the electrochemical reactions of the redox couples of I_2/I^- at the positive electrode, with reduction peak as a discharge process and oxidation as a charging process. All the positive electrodes show similar cyclic voltammetric curves with different current values. The cyclic voltammetric curves confirm that the redox reaction is occurred in the range, which we observed

(0.7 - 1.7 V). Besides, the CV curves show a single pair of oxidation-reduction peaks. Attributable, there are not the oxidation-reduction reactions of polymer binders in positive electrodes [19]. The results show the PVA-NaCMC positive electrode has the highest current and low peak separation between oxidation and reduction peak, indicating that the best electrochemical reaction activity and improve the zinc ion diffusion of a positive electrode among the electrodes processed with other binders.

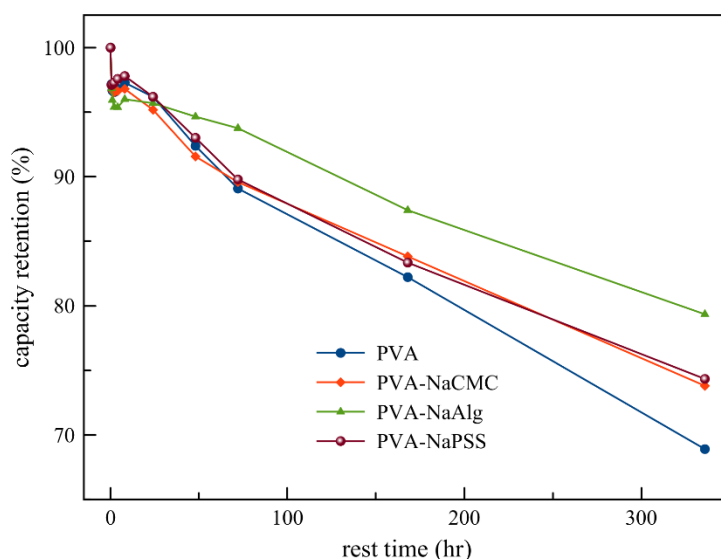


Figure 21 Self-discharge of batteries with different binders at various times rest in charge state.

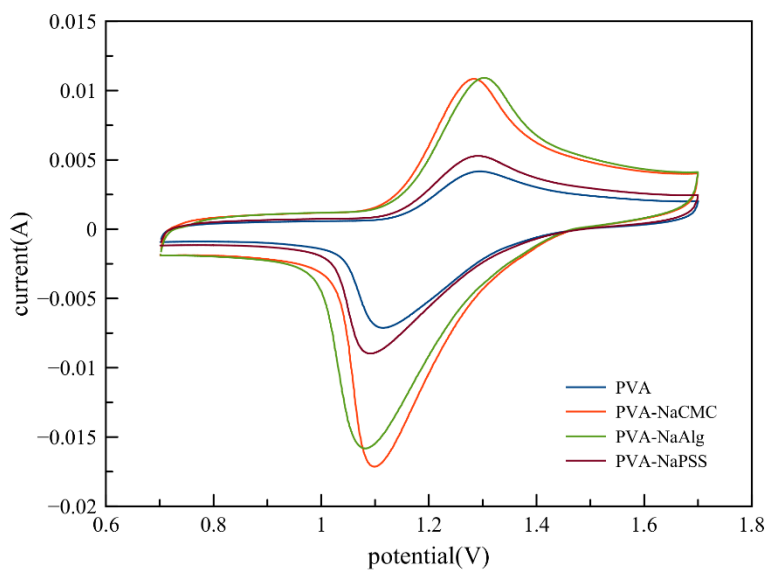


Figure 22 Cyclic voltammograms of the zinc-iodine batteries with positive electrode processed with different binders at a scan rate of 5 mV/s

To study the diffusion dynamics, the Nyquist plots at various charge/discharge state of the positive electrode with different binders are presented in Fig. 23 (a-d). The Nyquist plots of PVA, PVA-NaAlg, and PVA-NaPSS binders have appeared only single RC (a resistor and a capacitor in parallel) semicircle at high frequency, indicating that the contact between an electrolyte and a positive electrode surface (charge transfer resistance). In contrast, the PVA-NaCMC binder has two semicircles at a high and medium frequency, which identified charge transfer resistance and resistance of solid electrolyte interphase (SEI) film layer, respectively. The formation of an SEI film layer of a PVA-NaCMC binder was observed because this binder can uptake in electrolyte easier than other binders. Also, Bode plots in Fig 24 (a-h) show a similar trend with the Nyquist plots, which have a clearly single-phase angle shift of PVA, PVA-NaAlg, and PVA-NaPSS while PVA-NaCMC has a double-phase angle shift. The Warburg diffusion phenomena of Zn^{2+} on the positive electrode at low frequency with a diagonal slope line of 45° [9, 12, 19, 36, 38] has the same among four electrodes (at charge/discharge 50%). The lowest real impedance or resistance at low frequency (10 mHz) of the PVA-NaAlg positive electrode in the charge/discharge 50% state is presented. It can conclude that the positive electrode using the PVA-NaAlg binder shows a faster diffusion of Zn^{2+} . Moreover, PVA-NaCMC and PVA-NaPSS binders have a similar curve of semicircles at all charge/discharge states leading to constant almost resistant, even different state of charge and discharge. Therefore, positive electrodes with anionic polyelectrolytes as supportive binders are favorable for improving the cycling stability and rate capability of rechargeable zinc-iodine batteries than positive electrode processed with a pure PVA binder.

Figure 23 (e) shows a comparison between fresh batteries and batteries after charge/discharge test 1000 cycles of various binders in positive electrodes. Both of charge transfer and SEI resistance of the PVA-NaCMC and PVA-NaAlg binders have decreased when these batteries went through charge/discharge test 1000 cycles. The charge transfer resistance after 1000 cycles of battery with PVA binder increased tremendously. As a result, positive electrodes with anionic polyelectrolytes as supportive binders have satisfied kinetics of reactions on electrodes, which supports the reason why these binders improved the cycling stability and rate capability of rechargeable zinc-iodine batteries.

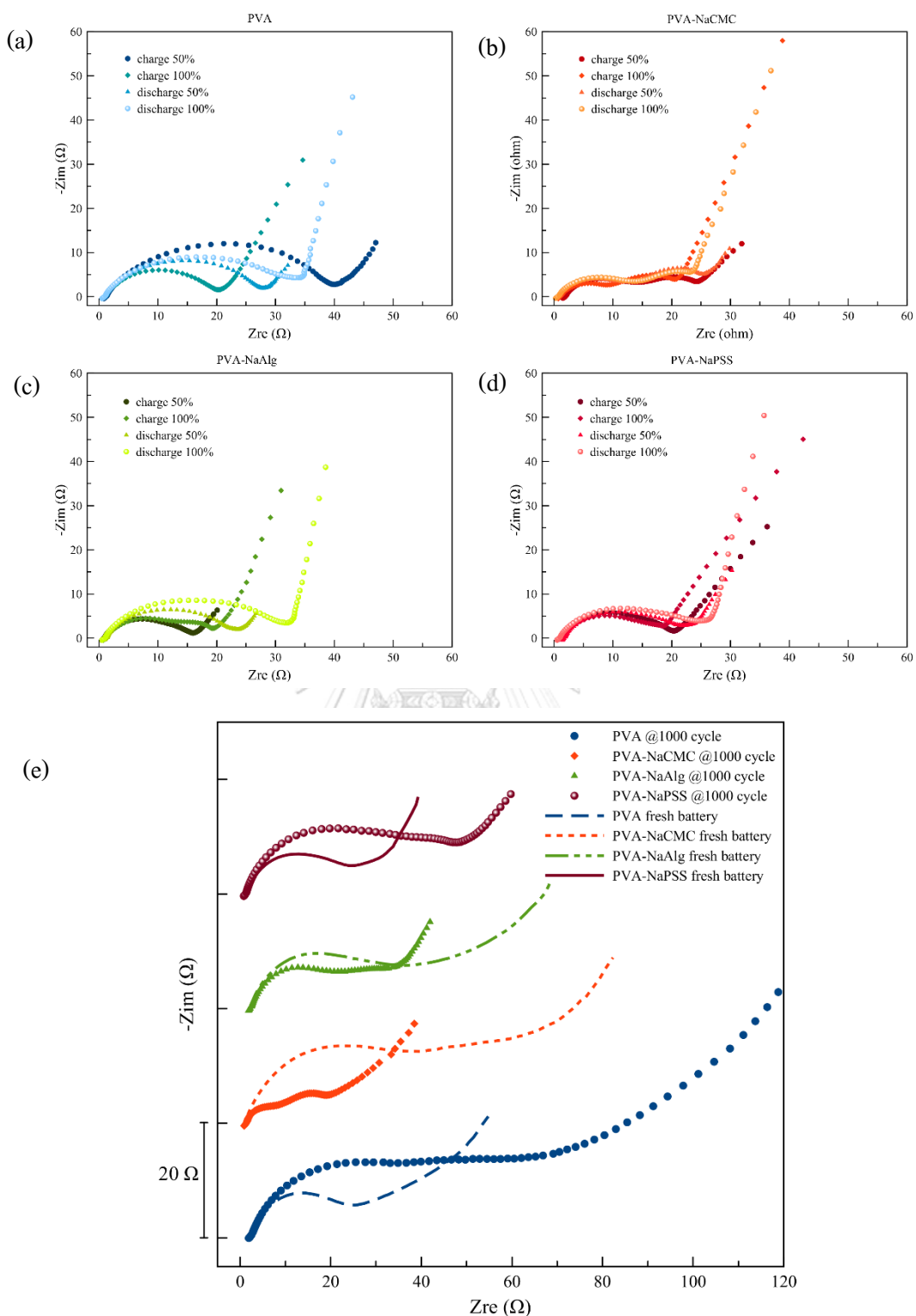


Figure 23 Nyquist plots of the positive electrode with (a) PVA, (b) PVA-NaCMC, (c) PVA-NaAlg, (d) PVA-NaPSS binders (at various charge/discharge state), (e) Nyquist plot comparing of fresh batteries and after 1000 cycles

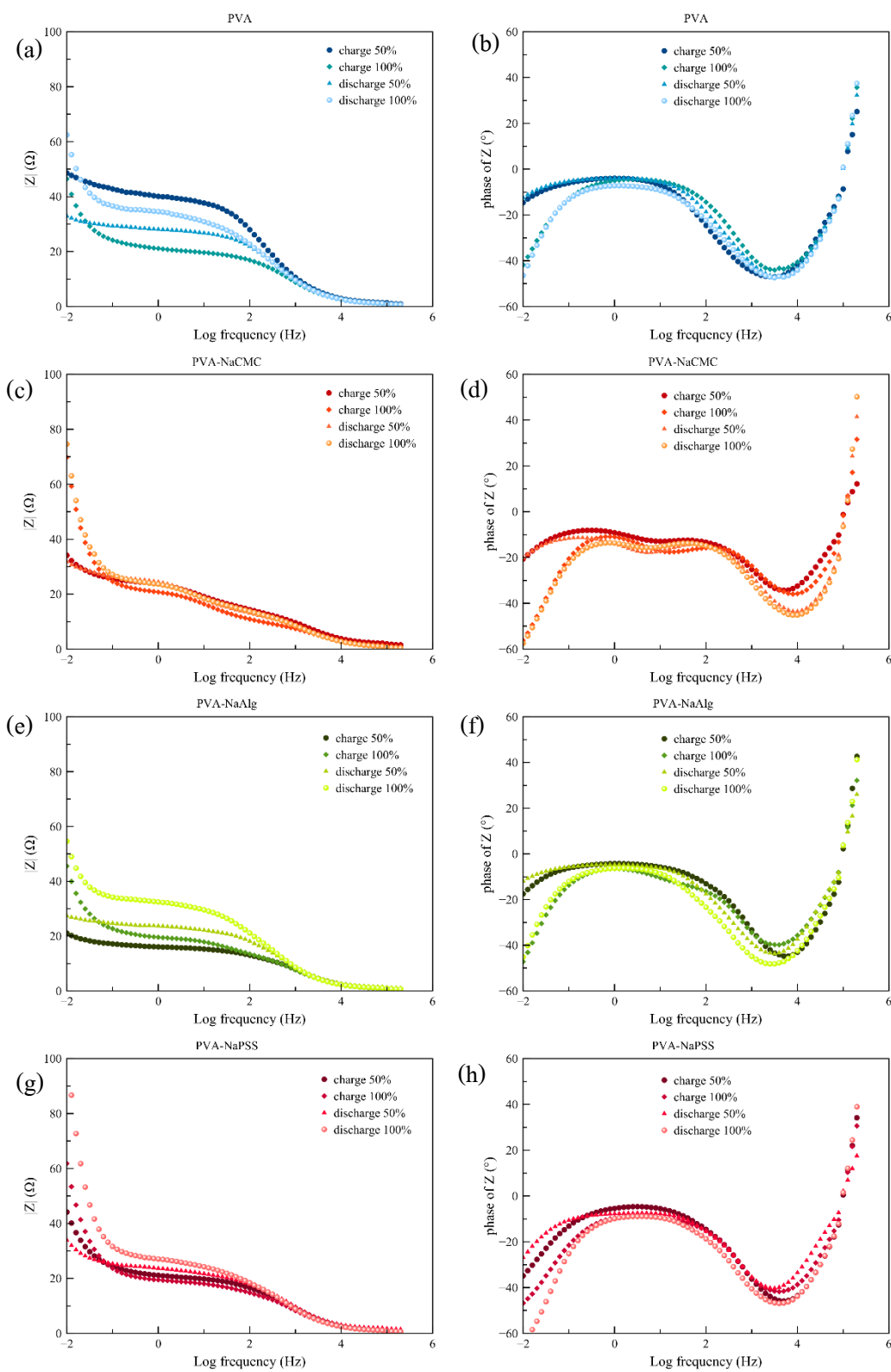


Figure 24 Bode plots of the positive electrode with (a,b) PVA, (c,d) PVA-NaCMC, (e,f) PVA-NaAlg, (g,h) PVA-NaPSS binders (at various charge/discharge state)

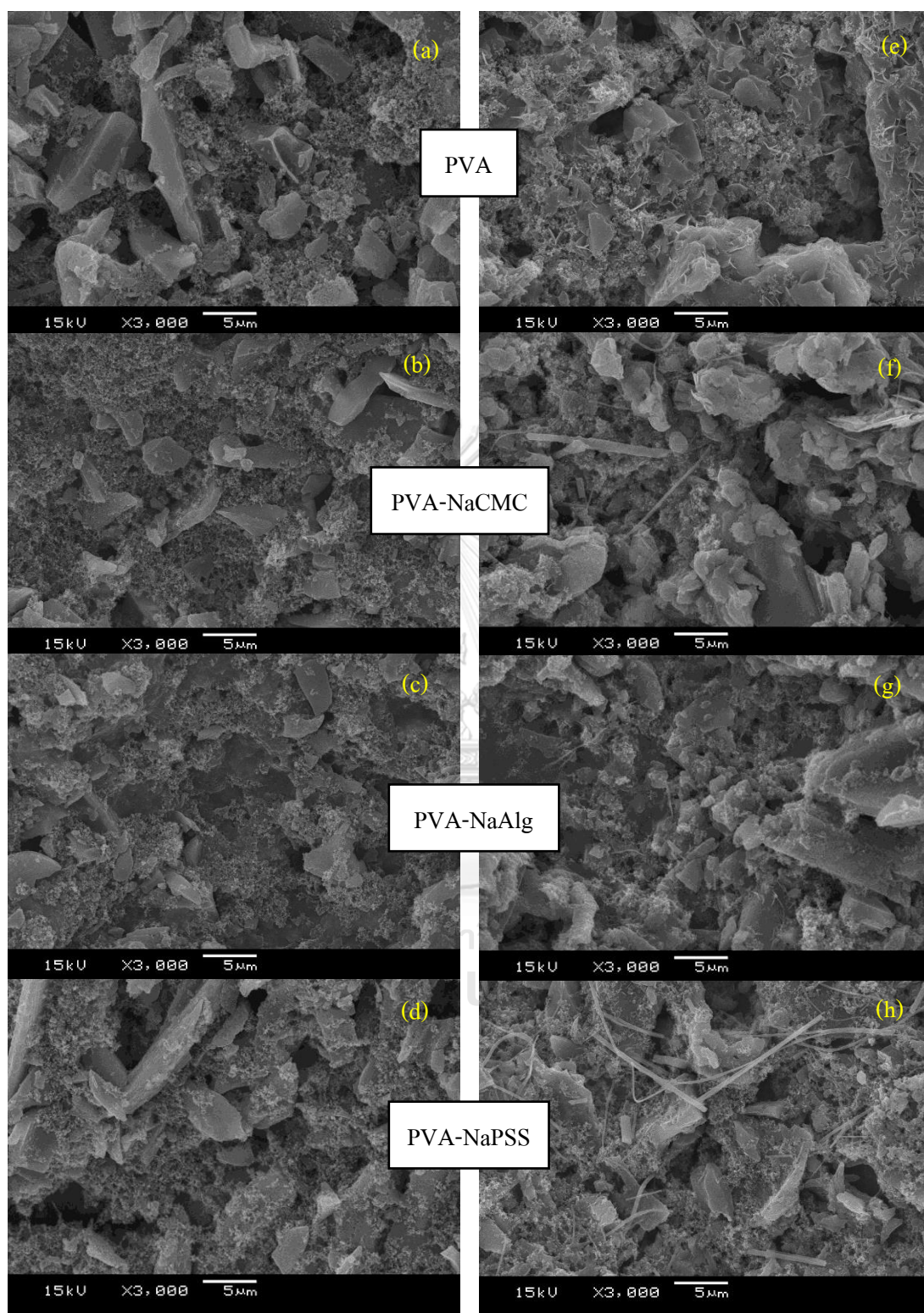


Figure 25 SEM image of positive electrode processed with PVA, PVA-NaCMC, PVA-NaAlg, and PVA-NaPSS binders (a, b, c, d) before the cycling test, (e, f, g, h) after 100 cycles

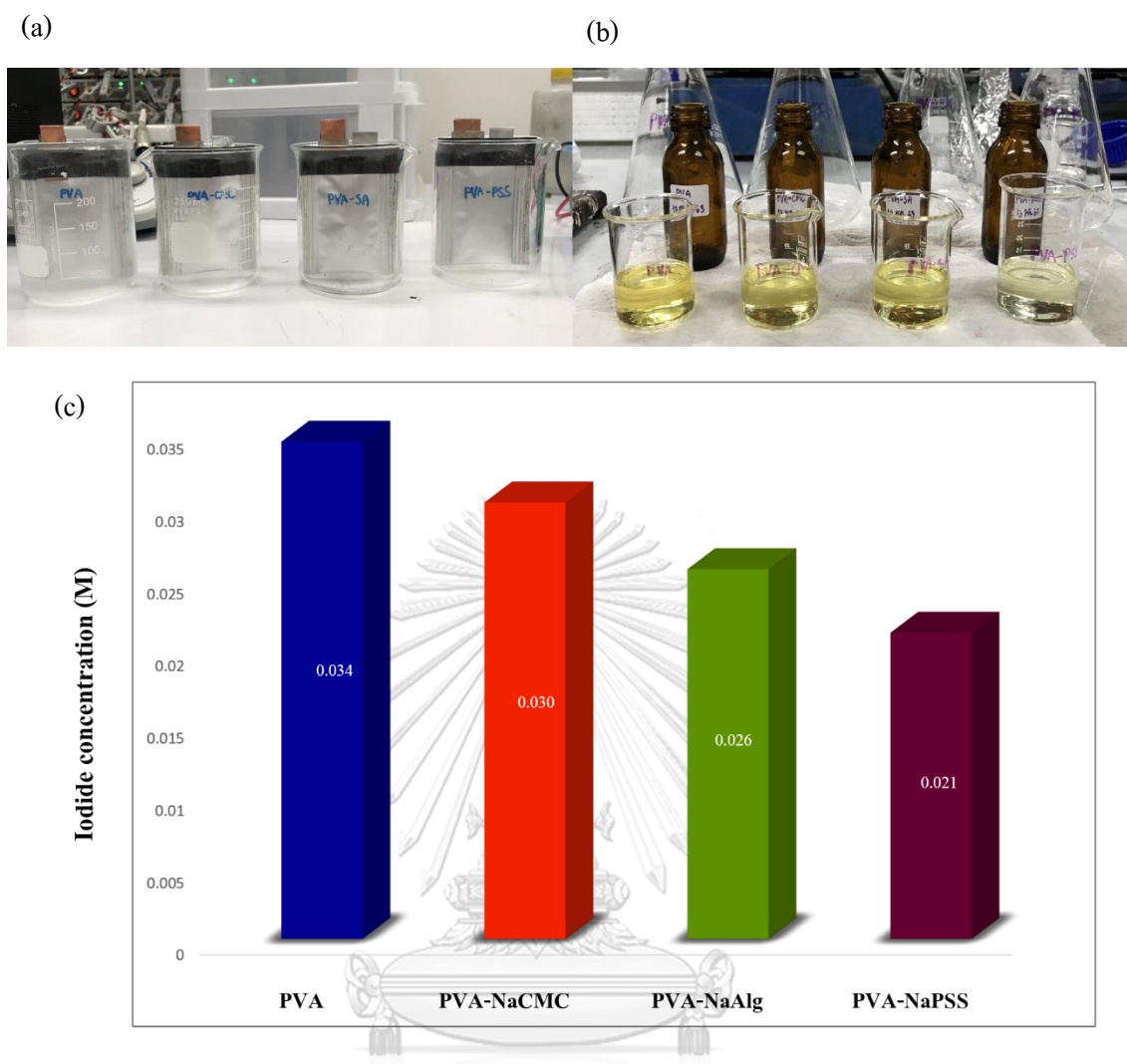


Figure 26 (a) pouch cell of the zinc-iodine batteries with positive electrode processed with different binders, (b) Electrolytes solution from pouch cell after charge/discharge ten cycles, (c) Iodide concentration diagram from titration of electrolyte.

To deeply investigate the reason why cycle performance and rate capability are different when using different binders. The SEM micrograph exhibited the physical morphology of positive electrodes processed with binders before and after charge/discharge 100 cycles, which was disassembled from batteries and dried before taking the image, as can be seen in Fig. 25 (a-h). The SEM images show active material and conductive agent distribution in binder networks, which are quite the same for both before and after 100 cycles in all positive electrodes, indicating these positive electrodes have high stability when used in zinc-iodine batteries system. The

positive electrodes after charge/discharge 100 cycles (Fig. 25 e-h) have little glass microfibers, which are from the separator of batteries after disassembly. Additionally, the positive electrodes processed with PVA-NaCMC, PVA-NaAlg, and PVA-NaPSS display high carbon conductive content surround active materials in binders network as mentioned in the previous part, indicating high electronic conductivity. Moreover, the uniform distribution and smooth surface lead to easy zinc ion diffusion in positive electrodes processed with these binders [12, 19]. As a result, the cycle performance and rate capability are excellent for using these anionic polyelectrolytes as supportive binders in rechargeable zinc-iodine batteries.

To confirm the encapsulation of iodine species by using anionic polyelectrolyte as supportive binders. Pouch cells, as shown in Fig. 26 (a) was fabricated, then charge/discharge test was performed at the current one mA/cm². After that, electrolytes in these cells were collected to titrate with silver nitrate (AgNO₃), which is presented in Fig. 26 (b) indicating the yellow color of iodine species dark shade from using a PVA binder to a light shade when using a PVA-NaPSS binder. Finally, the iodide concentration, as shown in Fig 26 (c), was obtained. The iodide concentration of using PVA, PVA-NaCMC, PVA-NaAlg, and PVA-NaPSS is 0.034, 0.030, 0.026, and 0.021 M, respectively, indicating that using these anionic polyelectrolytes as supportive binders give lower iodide concentration in electrolyte solution after charge/discharge test for 10 cycles. Therefore, these anion polyelectrolytes can encapsulate iodine species in positive electrodes lead to a low self-discharge rate [39, 40] and better electrochemical performance in these batteries.

Chapter V

Conclusion

In this work, using sodium carboxymethyl cellulose (NaCMC), sodium alginate (NaAlg), and sodium polystyrene sulfonate (NaPSS) as supportive binders in an aqueous solvent and prepared the positive electrodes for zinc-iodine batteries were studied. Since PVA has been used as a binder in a positive electrode [8], the binder films of PVA, PVA-NaCMC, PVA-NaAlg, and PVA-NaPSS have been studied to compare the performance in this study in which they are stable in the electrolyte, which can be noticed from maintaining binder film after electrolyte soaking. Electrolyte uptake of PVA-NaCMC reaches 127.38%, which is the highest value among the four binders, indicating that a PVA-NaCMC binder has preferably high ion conductivity. However, the morphology of a positive electrode processed with this binder displays better than other binders, noticing from the high electrical conductivity of the electrode with a value of 7297 S/m. Which using PVA-NaAlg and PVA-NaPSS binders, batteries show an excellent property as next-level regard from the PVA-NaCMC binder due to the high carbon conductive content surround active materials in the binder network. The uniform distribution and smooth surface lead to easier zinc ion diffusion in positive electrodes processed with these binders. As a result, the cycle performance and rate capability are excellent for using these anionic polyelectrolytes as supportive binders in rechargeable zinc-iodine batteries.

The zinc-iodine batteries in this study have high cycle performance, which reaches 1000 cycles. The initial specific discharge capacities of the PVA-NaCMC, PVA-NaAlg, and PVA-NaPSS positive electrode at a current rate 3C are 127.37 mAh g⁻¹, 114.14 mAh g⁻¹, 106.05 mAh g⁻¹, respectively. The specific capacity retentions of the PVA-NaCMC, PVA-NaAlg, and PVA-NaPSS positive electrode at the same current rate are 91.6%, 89.5%, and 92.6%, respectively. It can be observed that the PVA-NaCMC positive electrode has the highest specific discharge capacity. Moreover, it has the high-rate capability and low self-discharge rate. Meanwhile, the specific discharge capacity and specific capacity retention of the PVA positive electrode is 104.06 mAh·g⁻¹ and 90.5%, respectively. The CV and EIS results indicate that the positive electrode processed with PVA-NaCMC, PVA-NaAlg, and PVA-NaPSS binders have faster zinc ion diffusion and satisfy kinetics of reactions on electrodes.

Additionally, these anion polyelectrolytes can encapsulate iodine species in positive electrodes, which can be observed by titration an electrolyte after the test cycle. Therefore, positive electrodes with these anionic polyelectrolytes as supportive binders are favorable for improving the cycling stability and rate capability. These are promising binders for the positive electrode in the rechargeable zinc-iodine batteries.



Appendix

Experiments

Van de Pauw method

The positive electrodes processed with different binders were investigated electrical conductivity by using Van der Pauw method equipment.

	I (mA)	V43 (mV)	V43 (average)	V14 (mV)	V14 (average)	R12,43	R23,14
PVA	1	0.032		0.02			
	-1	-0.054	0.043	-0.028	0.024	0.043	0.024
	2	0.079		0.044			
	-2	-0.094	0.0865	-0.05	0.047	0.04325	0.0235
	3	0.12		0.068			
	-3	-0.138	0.129	-0.074	0.071	0.043	0.023667
	4	0.164		0.096			
	-4	-0.181	0.1725	-0.096	0.096	0.043125	0.024
	5	0.206		0.12			
	-5	-0.226	0.216	-0.117	0.1185	0.0432	0.0237
PVA-NaCMC	1	0.025		0.016			
	-1	-0.056	0.0405	-0.029	0.0225	0.0405	0.0225
	2	0.084		0.023			
	-2	-0.095	0.0895	-0.054	0.0385	0.04475	0.01925
	3	0.126		0.047			
	-3	-0.139	0.1325	-0.07	0.0585	0.044167	0.0195
	4	0.171		0.069			
	-4	-0.186	0.1785	-0.085	0.077	0.044625	0.01925
	5	0.215		0.092			
	-5	-0.23	0.2225	-0.1	0.096	0.0445	0.0192
PVA-NaAlg	1	0.032		-0.014			
	-1	-0.055	0.0435	-0.053	0.0195	0.0435	0.0195
	2	0.083		0.01			
	-2	-0.103	0.093	-0.074	0.042	0.0465	0.021
	3	0.13		0.021			
	-3	-0.146	0.138	-0.1	0.0605	0.046	0.020167
	4	0.18		0.04			
	-4	-0.19	0.185	-0.11	0.075	0.04625	0.01875
	5	0.22		0.08			
	-5	-0.24	0.23	-0.12	0.1	0.046	0.02
PVA-NaPSS	1	0.033		0.02			
	-1	-0.024	0.0285	-0.052	0.036	0.0285	0.036
	2	0.064		0.052	0.071	0.0295	0.0355

	-2	-0.054		-0.09			
	3	0.095		0.09			
	-3	-0.084	0.0895	-0.13	0.11	0.029833	0.036667
	4	0.124		0.126			
	-4	-0.113	0.1185	-0.163	0.1445	0.029625	0.036125
	5	0.154		0.164			
	-5	-0.142	0.148	-0.198	0.181	0.0296	0.0362

(Continuos)

	R23,14/R12,43 (Ω)	F(Q)	ρ ($\Omega \cdot m$)	ρ ($\Omega \cdot m$) (average)	σ (S/m)
PVA	1.791666667	0.98	0.000149		
	1.840425532	0.98	0.000148		
	1.816901408	0.98	0.000148	0.000148549	6731.7679
	1.796875	0.98	0.000149		
	1.82278481	0.98	0.000149		
PVA- NaCMC	1.8	0.95	0.000136		
	2.324675325	0.95	0.000138		
	2.264957265	0.95	0.000137	0.000137027	7297.8502
	2.318181818	0.95	0.000138		
	2.317708333	0.95	0.000137		
PVA- NaAlg	2.230769231	0.95	0.000136		
	2.214285714	0.95	0.000145		
	2.280991736	0.95	0.000142	0.000141085	7087.9349
	2.466666667	0.95	0.00014		
	2.3	0.95	0.000142		
PVA- NaPSS	1.263157895	1	0.000146		
	1.203389831	1	0.000147		
	1.229050279	1	0.000151	0.000148457	6735.9365
	1.219409283	1	0.000149		
	1.222972973	1	0.000149		

For measuring the resistivity gives equation

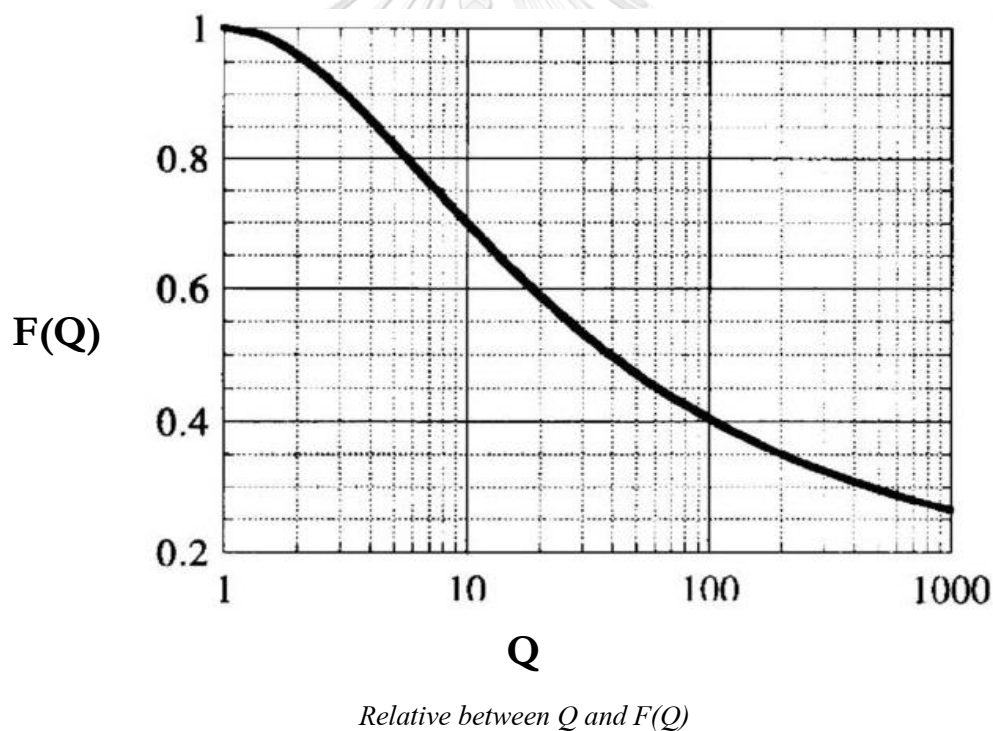
$$\text{Resistivity } (\rho) = \frac{\pi d}{\ln 2} \left(\frac{R_{12,43} + R_{23,14}}{2} \right) F(Q)$$

With $F(Q)$ is found by solving the equation:

$$\frac{Q-1}{Q+1} = \frac{F}{\ln 2} \cosh^{-1} \left(\frac{e^{\left(\frac{\ln 2}{F}\right)}}{2} \right)$$

When $R_{23,14} > R_{12,43}$

$$Q = \frac{R_{23,14}}{R_{12,43}}$$



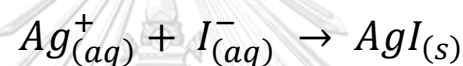
Iodide precipitation titrations

The pouch cell after 10 cycles charge/discharge test was disassembled to collect the electrolyte. The electrolyte was titrated with silver nitrate (AgNO_3) 0.05M and eosin 0.1%w/v as an indicator

The example of titration one series.

	V(initial)	V(final)	V(AgNO ₃ used)	mol of AgNO ₃	mol of I ⁻	Molar of I ⁻ (M)
PVA	0	9.6	9.6	0.00048	0.00048	0.048
PVA-NaCMC	10	14.4	4.4	0.00022	0.00022	0.022
PVA-NaAlg	15	16.9	1.9	9.5E-05	9.5E-05	0.019
PVA-NaPSS	17	18.5	1.5	0.000075	0.000075	0.015

The reaction of silver iodide shows as an equation.



Electrolyte uptake

Weighting the film before and after soaking in 2M ZnSO₄ for 24 hr. Calculate the percent of the increase in film weight to determine electrolyte uptake value.

	W(initial)(g)	W(final)(g)	%uptake
PVA	0.0262	0.0344	31.2977099
PVA-NaCMC	0.0084	0.0191	127.380952
PVA-NaAlg	0.0418	0.083	98.5645933
PVA-NaPSS	0.0135	0.0202	49.6296296

The equation of calculating electrolyte uptake value

$$\% \text{ electrolyte uptake} = \left(\frac{\text{Weight}_{\text{final}}}{\text{Weight}_{\text{initial}}} - 1 \right) * 100$$

REFERENCES

1. Root, M., *The TAB™ Battery Book* 2011: The McGraw-Hill Companies. 252.
2. Lu, K., et al., *Sulfur and Nitrogen Enriched Graphene Foam Scaffolds for Aqueous Rechargeable Zinc-Iodine Battery*. *Electrochimica Acta*, 2019. **296**: p. 755-761.
3. Li, H., et al., *Advanced Rechargeable Zinc-Based Batteries: Recent Progress and Future Perspectives*. *Nano Energy*, 2019. **62**: p. 550-587.
4. Bai, C., et al., *A Sustainable Aqueous Zn-I₂ Battery*. *Nano Research*, 2018. **11**(7): p. 3548-3554.
5. Yamamoto, T., *Use of Polymer-Iodine Adducts as Positive Electrodes of Cells* *J. Chem. Soc., Chem. Commun*, 1981: p. 187-188.
6. Yamamoto, T., M. Hishinuma, and A. Yamamoto, *Zn |ZnI₂ | Iodine Secondary Battery Using Iodine- Nylon-6 Adduct as Positive Electrode, and Its Charge-Discharge Performance* *Inorganica Chimica Acta*, 1984. **86**: p. 47-49.
7. Hishinuma, M., et al., *Zinc-Iodine Secondary Cell Using 6-Nylon or Poly(ether) Based Electrode Basic Research for Industrial Use of The Econdary Cell*. *Electrochimica Acta* 1990. **35**: p. 255-261.
8. Tedjar, F., *Multilayer Thin-Film Batteries With Poly(viny alcohol)* *Journal of Power Sources*, 1994. **48**: p. 285-291.
9. Wang, Z., et al., *CMC as A Binder in LiNi_{0.4}Mn_{1.6}O₄ 5V Cathodes and Their Electrochemical Performance for Li-ion Batteries*. *Electrochimica Acta*, 2012. **62**: p. 77-83.
10. Godoi, F.C., et al., *Dependence of LiNO₃ Decomposition on Cathode Binders in Li-S Batteries*. *Journal of Power Sources*, 2015. **288**: p. 13-19.
11. Bao, W., et al., *Enhanced Cyclability of Sulfur Cathodes in Lithium-Sulfur Batteries with Na-Alginate as A Binder*. *Journal of Energy Chemistry*, 2013. **22**(5): p. 790-794.
12. Yang, Z., R. Li, and Z. Deng, *Polyelectrolyte Binder for Sulfur Cathode to Improve The Cycle Performance and Discharge Property of Lithium-Sulfur Battery*. *ACS Appl Mater Interfaces*, 2018. **10**(16): p. 13519-13527.
13. Xie, C., et al., *A Long Cycle Life, Self-Healing Zinc-Iodine Flow Battery with High Power Density*. *Angew Chem Int Ed Engl*, 2018. **57**(35): p. 11171-11176.

14. Li, Y., et al., *Rechargeable Aqueous Zinc-iodine Batteries: Pore Confining Mechanism and Flexible Device Application*. Chem Commun (Camb), 2018. **54**(50): p. 6792-6795.
15. Li, B., et al., *Ambipolar Zinc-polyiodide Electrolyte for a High-energy Density Aqueous Redox Flow Battery*. Nat Commun, 2015. **6**: p. 6303.
16. Lee, J., et al., *Nanoconfinement of Redox Reactions Enables Rapid Zinc Iodide Energy Storage with High Efficiency*. Journal of Materials Chemistry A, 2017. **5**(24): p. 12520-12527.
17. Rajeswari, N., et al., *A Study on Polymer Blend Electrolyte Based on PVA/PVP with Proton Salt*. Polymer Bulletin, 2014. **71**(5): p. 1061-1080.
18. Chiellini, E., et al., *Biodegradation of Poly (vinyl alcohol) Based Materials*. Progress in Polymer Science, 2003. **28**(6): p. 963-1014.
19. Yang, S., et al., *Hybrid Humics/sodium Carboxymethyl Cellulose Water-Soluble Binder for Enhancing The Electrochemical Eerformance of A Li-ion Battery Cathode*. Powder Technology, 2019. **351**: p. 203-211.
20. Parks, M. and D. Grady, *Sodium Polystyrene Sulfonate for Hyperkalemia*. JAMA Intern Med, 2019.
21. Mbareck, C., Q.T. Nguyen, and M.J. Saiter, *Poly(vinyl alcohol) and Poly(sodium styrene sulfonate) Compatibility by Differential Scanning Calorimetry, Fourier Transform Infrared and Scanning Electron Microscopy*. Journal of Applied Polymer Science, 2009. **114**(4): p. 2261-2269.
22. Ngo, N., et al., *Van der Pauw Resisitivity Measurement*. 2017: ResearchGate.
23. Van der pauw, L.J., *A Method of Measuring the Resistivity and Hall Coefficient on Lamellae or Arbitrary Shape*. Philip Technical Review, 1958. **20**: p. 220-224.
24. Najmudin, Z., *The Hall Effect*. 2014.
25. Kaiho, T., *Iodine Chemistry and applications*. 2015: John Wiley & Sons. 636.
26. *Precipitration Titration*. p. 340-356.
27. *Testing Electrochemical Capacitors Part 1: CV, EIS, And Leakage Current*. GAMRY instrument.
28. *Basics of Electrochemical Impedance Spectroscopy* 2010: GAMRY instrument.
29. Harrington, D.A. and P. Van den Driessche, *Mechanism and Equivalent Circuits in*

- Electrochemical Impedance Spectroscopy*. *Electrochimica Acta*, 2011. **56**(23): p. 8005-8013.
30. Benavente, J., *Electrochemical Impedance Spectroscopy as a Tool for Electrical and Structural Characterizations of Membranes in Contact with Electrolyte Solutions*, in *Recent Advances in Multidisciplinary Applied Physics*. 2005. p. 463-471.
 31. Promsila, W., *Karn Seaksa Impedance Spectroscopy Seang Kamee Firefah Kong Polyaniline Somrub Wad Karn Num Firefah Bab Mai Sarub [Electrochemical Impedance Spectroscopic Study of Polyaniline Sensor for Contactless Conductivity Measurement]*. 2013, Rajamangala University of Technology Krungthep. p. 49.
 32. Li, J., C. Daniel, and D.L. Wood, *Cathode Manufacturing for Lithium-Ion Batteries*, in *Handbook of Battery Materials* 2011: Wiley-VCH. p. 939-960.
 33. Yoo, s., et al., *Analysis of Pouch Performance to Ensure Impact Safety of Lithium-Ion Battery*. *Energies*, 2019. **12**(15).
 34. Cheng, M., et al., *A Novel Binder-Sulfonated Polystyrene for The Sulfur Cathode of Li-S Batteries*. *Ionics*, 2017. **23**(9): p. 2251-2258.
 35. Pimalai, D., *Karn Seaksa Yang Tummachart Pen San Yudkoa Nai Kour Anode Chanid Silicon Somrub Battery lithium-Ion [Investigation of Natural Rubber as A Binder for Silicon Anode in Lithium-ion Batteries]*, in *Department of Chemical Engineering Faculty of Engineering*. 2017, Thammasat University
 36. Francesca, B., et al., *Sodium Alginate: A Water-Processable Binder in High-Voltage Cathode Formulations*. *Journal of The Electrochemical Society*, 2016. **164**(1): p. A6171-A6177.
 37. Wang, Y., et al., *Enhancing Electrochemical Properties of Graphite Anode by Using Poly(methylmethacrylate)–Poly(vinylidene fluoride) Composite Binder*. *Carbon*, 2015. **92**: p. 318-326.
 38. Sun, J., et al., *Effect of Poly (acrylic acid)/Poly (vinyl alcohol) Blending Binder on Electrochemical Performance for Lithium Iron Phosphate Cathodes*. *Journal of Alloys and Compounds*, 2019. **783**: p. 379-386.
 39. Zhao, Q., et al., *Rechargeable Lithium-Iodine Batteries with Iodine/Nanoporous Carbon Cathode*. *Nano Lett*, 2015. **15**(9): p. 5982-7.

40. Zhang, G., et al., *Using Core–Shell Interlinked Polymer@C–Iodine Hollow Spheres to Synergistically Depress Polyiodide Shuttle and Boost Kinetics for Iodine-Based Batteries.* *Journal of Materials Chemistry A*, 2018. **6**(19): p. 9019-9031.



VITA

NAME Jirapha Pimoei

DATE OF BIRTH 28 November 1995

PLACE OF BIRTH Mahasarakham, Thailand

INSTITUTIONS ATTENDED B.S. Industrial Chemistry Faculty of Science at Kasetsart
University

HOME ADDRESS 268 Village No. 3, Non Rasi Subdistrict, Borabue District, Maha
Sarakhm Province 44130

PUBLICATION The 29th Thai Institute of Chemical Engineering and Applied
Chemistry Conference (TICChE2020), 1-2 June 2020. Iodine
Encapsulation Using Anionic Polyelectrolyte for Rechargeable
Zinc-iodine Batteries. page 87-93.